Quantifying the present and future environmental sustainability of cleanrooms

Cell Reports
Sustainability

Article

Quantifying the present and future environmental sustainability of cleanrooms

Graphical abstract

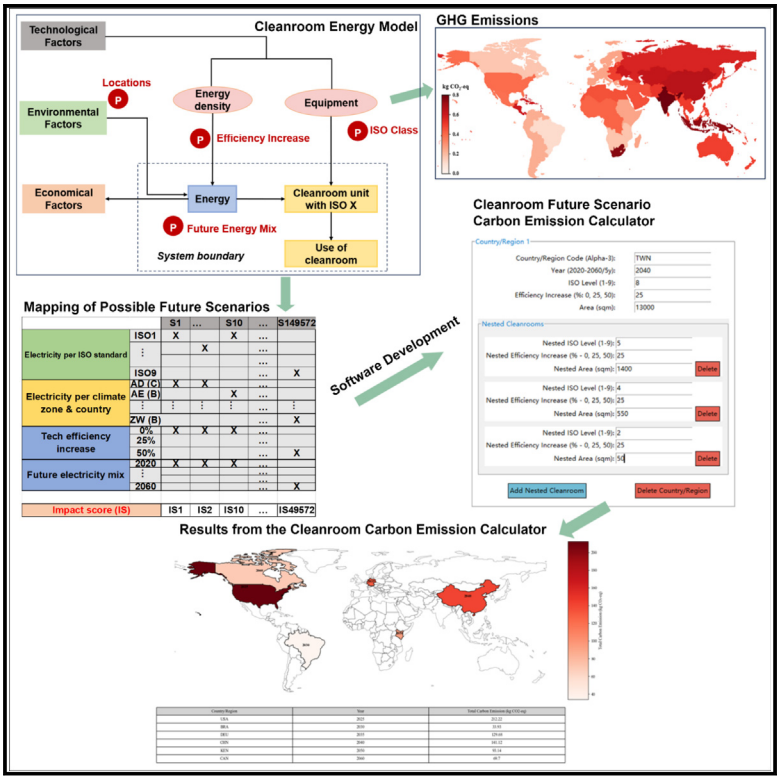

Highlights

- Environmental sustainability of cleanrooms under future conditions is studied
- 68 trillion indicator results are obtained to identify suitable cleanroom locations
- Publication of usable data and scenarios to support LCA analysis for cleanrooms

Authors

Justin Z. Lian, Flora Siebler, Bernhard R.P. Steubing, ..., Karl Leo, Indraneel Sen, Stefano Cucurachi

Correspondence

s.cucurachi@cml.leidenuniv.nl

In brief

Lian et al. introduce a modeling framework to assess cleanroom energy use and emissions under future climate scenarios. By evaluating 49,572 scenarios, the study emphasizes the importance of planning for optimized cleanroom operations, reducing greenhouse gas emissions, and mitigating climate impacts. This work provides insights for developing sustainable cleanroom practices across various industries. A cleanroom carbon emission calculator has been developed to assist users in locating scenarios of interest more effectively by inputting criteria into the models.

Lian et al., 2024, Cell Reports Sustainability *1*, 100219
September 27, 2024
https://doi.org/10.1016/j.crsus.2024.100219

CellPress

Cell Reports Sustainability

CellPress
OPEN ACCESS

Article

Quantifying the present and future environmental sustainability of cleanrooms

Justin Z. Lian,[1,6] Flora Siebler,[1,6] Bernhard R.P. Steubing,[1] Aldo Jesorka,[2] Valerio Barbarossa,[1,3] Ranran Wang,[1] Karl Leo,[4] Indraneel Sen,[5] and Stefano Cucurachi[1,7,*]

[1]Leiden University, Institute of Environmental Science – Industrial Ecology, Van Steenisgebouw, Einsteinweg 2, 2333 CC Leiden, the Netherlands

[2]Department of Chemistry and Chemical Engineering, Chalmers University of Technology, 412 96 Göteborg, Sweden

[3]PBL Netherlands Environmental Assessment Agency, The Hague, the Netherlands

[4]Dresden Integrated Center for Applied Physics and Photonic Materials (IAPP), Technische Universität Dresden, 01062 Dresden, Germany

[5]Wasabi Innovations Ltd., Boulevard Tsarigradsko Shose, No. 111B, Building Incubator, 1784 Sofia, Bulgaria

[6]These authors contributed equally

[7]Lead contact

*Correspondence: s.cucurachi@cml.leidenuniv.nl

https://doi.org/10.1016/j.crsus.2024.100219

SCIENCE FOR SOCIETY Cleanrooms are critical infrastructure for high-precision industries such as semiconductors and microelectronics. However, rigid control over temperature, humidity, airflow, etc. requires high energy consumption, which can vary significantly with local climate factors. Given the potential impact of near-future climatic changes, it becomes increasingly important to study the operation of cleanrooms in future scenarios. Our approach combines the quantitative assessment of cleanroom sustainability in space and time with an analysis of how energy consumption and local climate shape environmental performance, enabling decision-makers with tools to identify suitable locations for cleanroom development based on fewer greenhouse gas emissions and climate impact. This study introduces a cleanroom energy demand modeling framework that integrates multiple data sources and employs advanced simulation techniques to address the complexities of cleanroom operations under varying climatic conditions.

SUMMARY

We investigated future cleanroom energy consumption by examining parameters, such as cleanroom class, electricity mix, technical efficiency, and location. These parameters were integrated with life cycle inventory (LCI) data and Integrated Model to Assess the Global Environment (IMAGE) regions, combining shared socioeconomic pathways (SSPs) and representative concentration pathways (RCPs) to calculate the carbon emissions. For various climatic zones, we considered heating and cooling degree days to estimate the energy consumption to maintain targeted temperatures. Therefore, we quantified the full spectrum of climate change impacts related to cleanroom operations across the globe and under future scenarios by evaluating 49,572 operational scenarios at the country level and 243 impact indicator maps, totaling over 68 trillion results from 2020 to 2060. Our findings stress the importance of strategic location for optimizing cleanroom operations. In applying our model, a scenario carbon emission calculator was developed to assist users in locating scenarios of interest more effectively by inputting their criteria into our models.

INTRODUCTION

Chips and microchips, some of the most technologically intensive and structurally sophisticated industrial products, are broadly implemented in a variety of electronic devices.[1] It is well acknowledged that the manufacturing process, particularly in advanced nanoscale dimensions, is exceedingly sensitive to impurities.[1,2] Airborne particles of critical size; contaminants in chemicals used in the chip-manufacturing process; pollutants in compressed air; the water used for cleaning, dilution, and reagents; impurities in the wafer materials; and other contamination may all contribute to chip flaws by influencing their mechanical, electrical, optical, and magnetic properties.[3,4] Therefore, chip manufacturing must be performed in clean and stable environments provided by cleanrooms.[5] In these facilities, the density of floating airborne particles is maintained within a defined range. In addition, cleanrooms allow strict control of temperature, humidity, air exchange rate, pressure difference,

electrostatic interactions, vibration, noise, and other relevant local operation conditions.[6–8] Without such a controlled environment, the chip-manufacturing process would be challenging at every stage, reducing yield or even preventing the fabrication of advanced devices.

In addition to the semiconductor sectors, cleanrooms are building blocks/key facilities in life science-related production processes and for developing emerging technologies and continuous innovation.[5] Cleanrooms, initially established in the semiconductor production sector, have nowadays a much wider range of applications. They are indispensable in modern technological endeavors, specifically in the preparation of biological materials,[9] pharmaceutical manufacturing,[10] food-related industries,[5] optics laboratories,[5] operating rooms in hospitals,[11] and generation of energy-transition products (solar photovoltaic panel manufacturing),[12] and others. Noteworthy are also applications in the fast-developing aerospace sector, sensitive instrumentation in safety-relevant aircraft applications, sensors, and the particularly expensive satellite and space exploration equipment, all of which cannot succeed without dedicated clean environments. Depending upon the nature of specific ventures and industries and prerequisites for the workplace, the cleanliness of the encased space of cleanrooms is classified into International Organization for Standardization (ISO) levels 1–9 by the international standards ISO 14644-1.[5,13–15] Although higher numbers indicate less stringent control parameters in the classifications, all levels have well-defined and standardized requirements. The details of the ISO levels can be found in Table S1.

The airflow in a cleanroom is fundamental for the undesired circulation and distribution of airborne particles of various sizes. These particles can never be completely eliminated but are greatly reduced in size ranges that negatively impact production processes. From a technical perspective, cleanrooms generally involve laminar flow and turbulent flow circulation modes. Higher-class cleanrooms commonly adopt laminar flow modes, also known as one-way flow (vertical or parallel flow) cleanrooms, which maintain cleanliness through continuous air exchange.[16,17] The treated clean air moves uniformly in one direction, either vertically or horizontally, over the entire block and displaces the existing air, which is driven out of the cleanroom and recirculated after filtering. In this case, clean airflow permeates the entire space rather than only a few outlying places. Turbulent flow is routinely used in lower-class cleanrooms. When fresh, purified air from the air supply enters the room, purified air spreads swiftly and mixes with the previous air, while approximately the same quantity of air is expelled through the return air outlet.[11,18–21] Thus, the clean airflow dilutes interior pollution and flushes down the initial dust concentration. Faster airflow dispersion allows for a more uniform and greater dilution effect.

By contrast, a laminar flow cleanroom has a substantially larger air supply volume than a turbulent one, allowing for greater cleanliness.[19,20] The ambient air is uniformly displaced by incoming air, typically called the "piston effect."[22] Both vertical and horizontal airflow regimes are applied, the former typically in fabrication cleanrooms and the latter in operation theaters and aerospace assembly facilities. As a result, the cost of constructing and maintaining a laminar flow cleanroom is markedly greater as it involves higher equipment investment and greater energy consumption.[23,24] In addition, integrating comprehensive air distribution strategies, effective filtration, and accommodating user-induced disturbances are essential for optimizing cleanroom energy consumption and operational efficiency.[8,25,26] Properly balancing these elements can lead to significant energy savings while maintaining the strict cleanliness standards required in cleanroom environments.

From the point of view of environmental sustainability, cleanrooms demand considerable energy regardless of class. This is due to the requirement to maintain a constant working environment with controlled temperature, humidity, regular air exchange rates and pressure differences, and other factors.[6] Cleanrooms may expend 30–50 times the energy of commercial buildings and even 100 times the energy of office buildings.[27,28]

Typically, cleanroom designers have been focusing on ensuring constant cleanliness as defined by the permitted particle count, additional requirements from the customer, and possibly energy efficiency and low maintenance costs. Rarely have manufacturers and users considered the overall sustainability of the system and how, for example, local variations such as different climates or means of electricity production might affect its environmental performance. Undoubtedly, the development of technology and management of technical efficiency (the efficiency with which a technology converts fuel into usable energy) could significantly increase energy efficiency and savings. For example, diminishing the air exchange rates outside of operational hours could effectively reduce energy consumption as industrial cleanrooms typically operate 24/7 for the whole year. This is a somewhat limited source of savings, perhaps even limited to research facilities.[29] In addition, moving forward with the decarbonization of the electricity mix (the variety and proportion of different energy sources used to generate electricity in a given region or country) could be another strategy from the standpoint of energy generation, although this factor is highly dependent on regions and policies.

Life cycle assessment (LCA)[30–33] is the current method of choice to assess the sustainability of products and technology systems that are connected to the global economy, such as cleanrooms. However, the absence of standardization in the design of cleanrooms poses a severe challenge for LCA analysts, who can rely on only a handful of dated sources, restricted life cycle inventory (LCI) data, and limited studies involving genuine measurement data. Such challenges do not allow an LCA analyst to effectively anticipate, forestall, or minimize the environmental impacts of emerging technologies that require cleanrooms. Unlike conventional LCA (or ex-post LCA), ex-ante LCA focuses on products or services with lower technology readiness levels (TRLs).[34–36] Ex-ante LCA studies use scenarios and models to describe and quantify possible future outcomes.[34,37] The results of such studies can support decision-making for sustainability at the earliest stages of decision- and policy-making and innovation.[30,38]

In this work, we assessed the environmental sustainability of cleanrooms under various climate and energy scenarios. To this end, we designed a flexible, modular tool to assess systems that are spatially distributed and bound to change over time due

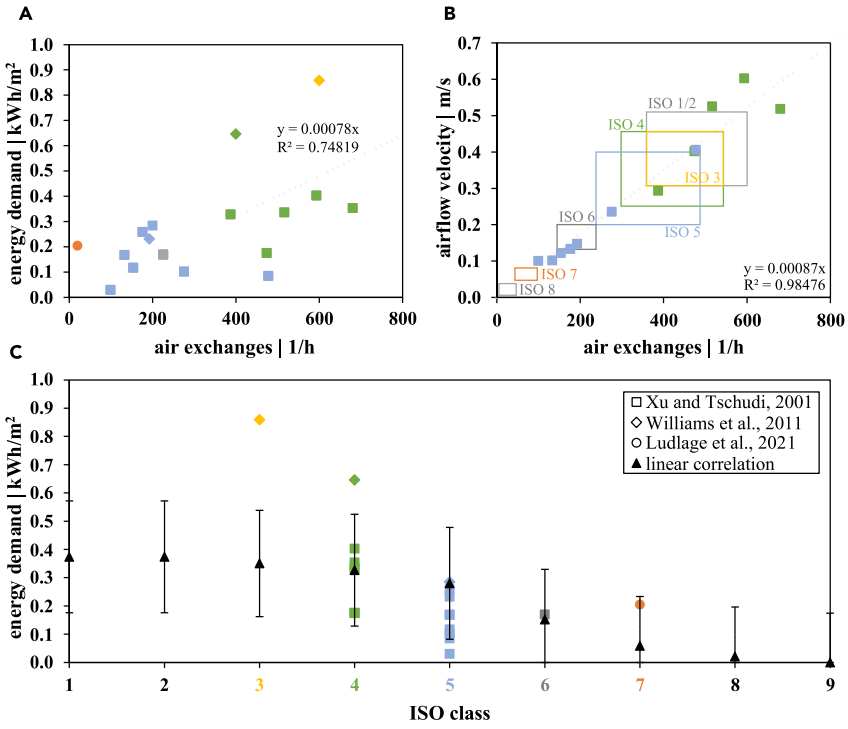

Figure 1. Energy demand needed for each cleanroom ISO class

The correlation is based on the data of Xu and Tschudi[43] for ISO 4 and ISO 5, Williams et al.[44] for ISO 3, ISO 4, and ISO 5, and Ludlage et al.[45] for ISO 7. Subplot (A) shows the linear regression between energy demand and air exchanges, and subplot (B) the recommendations (boxes) of IEST-RP-CC012.1[42] for each cleanroom ISO class. The final correlation between all ISO classes and the energy demand (black triangles) is shown in (C). Linear regression errors combined with IEST-RP-CC012.1 recommendation variance are also displayed.

to climate-related and economic factors. Four main parameters related to cleanroom electricity consumption were defined and studied: *electricity per ISO standard* (P1), *electricity per climate zone* (P2), *technical efficiency increase* (P3), and *future electricity mix* (P4). Our research has revealed that climate zones significantly affect cleanroom electricity consumption. From our wafer fab cleanroom scenarios studies and examples from Taiwan Semiconductor Manufacturing Company's (TSMC) fabs (based on its published data), the influence of climate zones could even account for over 40% of cleanroom electricity usage, and choosing the right construction climate zone could save about 20% of electricity. Moreover, studying the impacts of climate zones on controlled environments is crucial for understanding the specific benefits related to cleanrooms and broader energy-saving applications. This research specifically contributes to the energy optimization discussion by demonstrating how cleanroom construction and lifetime operations can benefit from adapting to different climate zones, considering all selected factors. Additionally, this research serves as a starting point for sustainability assessments of other high-specification systems or buildings with high energy demands that depend on specific local operation conditions.[39–41] This is particularly relevant within the framework of sustainable development and sustainability by design.

RESULTS

Energy demand per ISO standard (P1)

Our analysis reveals a linear correlation between energy demand and air exchanges necessary to maintain specific cleanroom ISO standards, as depicted in Figure 1A with a gray dotted line. Figure 1 provides an overview of deriving parameter P1, electricity consumption per ISO standard, and Figure 1B illustrates the IEST-RP-CC012.1 (Institute of Environmental Sciences and Technology-Recommended Practice [IEST-RP]) guidelines[42] for air change and airflow velocity ranges, as per Xu and Tschudi's findings[43] denoted by square boxes.

The distinct characteristics of ISO classes 4 and 5 are evident from the analysis, where significant differences in air exchange and airflow velocity appeared as key factors in distinguishing these classes, as can be seen in Figures 1A and 1B. By establishing a linear correlation between energy demand and air exchange rate, we generalized the energy requirements across various ISO classes. This approach combined with the average cleanroom guidelines from IEST-RP-CC012.1[42] allows us to calculate the average energy consumption for each classification, as detailed in Table S2. An S-shaped relationship between ISO class and electricity usage was identified, peaking at approximately 0.37 kWh/m^2 with a notable decrease in average energy demand, particularly between ISO 5 and ISO 6, as depicted in Figure 1C. As for ISO 9, because there are no specific requirements for airflow velocities or air change rates according to the ISO standards, these data were not available, as listed in Tables S1 and S2 for ISO 9. Therefore, for ISO 9 in this study, only the energy for temperature control (heating and cooling) was calculated. Variances in energy demand were illustrated by error bars and were derived from combining linear regression error with the variance in IEST-RP-CC012.1 recommendations. Incorporating data from studies conducted in the United States and the Netherlands,[43] we formulated a weighted average for heating and cooling energy demands (as elaborated in the experimental procedures part and Table S2, P1 range), resulting in a final P1 range that precisely quantifies electricity usage for each ISO class, independently of the energy required for temperature control.

Energy demand per climate zone (P2)

To assess the influence of cleanroom location on energy requirements, we analyzed the energy needed to maintain specific temperatures, denoted as parameter P2. Our findings showed that on average, heating degree days (HDDs) exceeded cooling

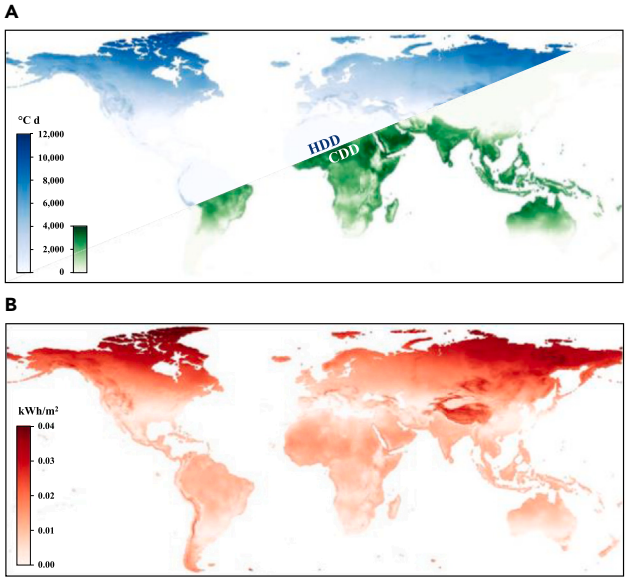

Figure 2. Annual heating and cooling degree days information

Annual heating and cooling degree days derived from spatial climate data (A) and energy demand needed to maintain a controlled temperature (B). In (A), the annual heating and cooling degree days (HDD and CDD, respectively, in °C) are shown. Their corresponding energy demand Q_{total} is visualized in (B). Both graphics are based on climate data for the time period 2021–2040 (see Table S3).

degree days (CDDs). A trend (see Figure 2A) was attributable to the threshold temperatures selected for HDDs and CDDs calculation, which was aligned with a global average temperature notably lower than the 18°C threshold. We calculated the total energy consumption for heating and cooling, Q_{total}, by applying HDD and CDD energy demand correlations shown in Figure 2B.[46] Both Figures 2A and 2B were based on climate data for the time period 2021–2040 (see Table S3 for spatiotemporal data sources and parameters for future scenarios).

The Köppen-Geiger climate zones (A–E level) and their global percentage share are represented in Figure 3A to highlight the distribution of different climate types. The total energy consumption, Q_{total}, for each climate zone (A–D) varies significantly, as detailed in Table S4 and depicted in Figure 3B. Figure 3C illustrates the proportion of the area of each climate zone relative to the total terrestrial surface in terms of providing insight into the global distribution of these climates. An analysis presented in Figure 3D indicates the contribution of heating and cooling to the total energy demand across these zones. In tropical (zone A) and arid (zone B) climates, the average energy demands are similar, yet air conditioning is predominantly required in the former, whereas heating might also be mandatory throughout the year in the latter. In temperate climates, there are generally fewer HDDs and CDDs, and the energy consumption for heating and cooling tends to be more balanced. Figure S1 further breaks down these aggregated climate zones by country along with the corresponding Q_{total} for each country to provide a comprehensive view of the geographical variation in energy demands for cleanrooms. However, polar zones (zone E) cover 37% of all lands and are characterized primarily by mountains, Greenland, and Antarctica, and these remote areas are generally unsuitable and unrealistic for cleanroom locations. Consequently, these zones were excluded from further depiction in our maps and statistical graphs.

Impact, threshold, and morphospace reduction (including technical efficiency increase, P3)

Utilizing our model to assess the energy consumption potential of cleanrooms with specific ISO standards in various regions, we conducted an illustrative scenario impact screening for ISO 5 cleanrooms, anticipating a 25% efficiency increase by 2030 at the regional level. The scenario revealed a range of climate change impact values from 0.0231 to 0.1644 kg CO_2-eq based on the Intergovernmental Panel on Climate Change (IPCC, global warming potential [GWP] 100a) midpoint method, as shown in the aggregation by country in Figure 4A, where scarlet indicates higher values. Additionally, we presented the impact as a year-by-year matrix from 2020 to 2060, which focused on the regional electricity mix of Western and Central Europe, as shown in Figure 4B. This figure highlights the impacts of climate change with different color scales used in each panel for value representation. Notably, most of Western Europe falls between 0.068 and 0.070 kg CO_2-eq, while several areas in Central Europe exceed this threshold, as indicated by the gray regions that mark values beyond our set threshold of 0.070 kg CO_2-eq.

If a decision-maker wished to use a screening criterion to rapidly remove unsustainable options, they could use these results to focus on specific areas to determine whether, for example, semiconductor manufacturing facilities in Europe would be appropriate in terms of sustainability. As an illustration, an impact threshold of 0.098 kg CO_2-eq (75th percentile of all scenarios in Figure 4D) was used in Figure 4C; the white area shows that the region was over the threshold and, therefore, was filtered out. Figure 4D shows the impact indicator distribution for all national data (dark gray) and ISO 5 (light gray), as well as the applicable thresholds (0.070–0.098 kg CO_2-eq, red dashed line).

The results indicate that the kg CO_2-eq (greenhouse gas [GHG]) emissions levels in the ISO 5, 2030, 25% scenario for Western and Central Europe are below the established environmental thresholds. Moreover, due to the emissions being significantly lower in Western Europe, it presents a more favorable location for establishing cleanrooms compared with Central Europe. If long-term development (from 2035 to 2060) and advancements in energy technology efficiency (from 25% to 50%) are considered, more and more countries and regions will likely be suitable for cleanrooms with the same criteria and standards. Of course, the users may also employ all the scenarios outlined in this study to assess whether developing a cleanroom in a specific country or region is sufficiently sustainable based on the analysis presented above. The full results of the scenarios from this research are available as shape files and Excel files in aggregated form per country and Integrated Model to Assess the Global Environment (IMAGE) region in the supplemental information.

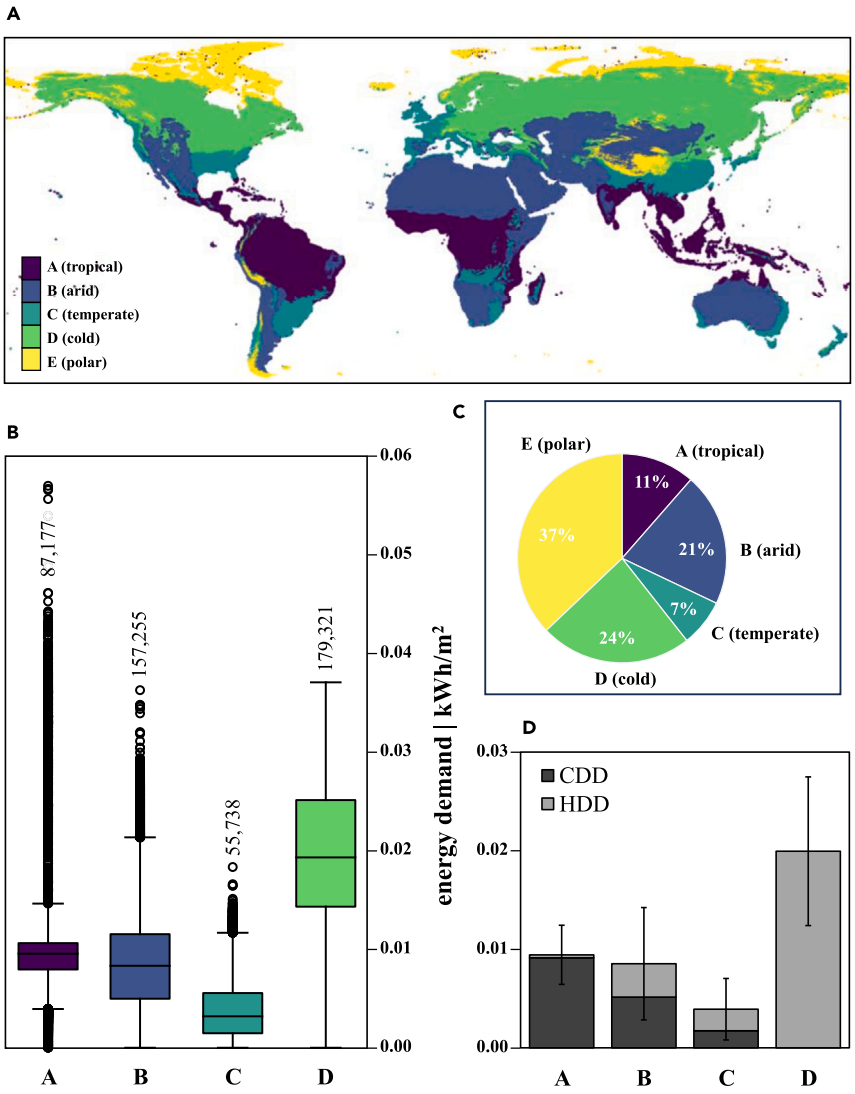

Figure 3. Energy demand per climate zone

(A) In (A), the Köppen-Geiger climate groups A–E without precipitation and heat levels are presented (historical data from Beck et al.,[47] Antarctica and Greenland are not shown). The distribution of the energy demand for heating and cooling per climate zone is depicted in (B). The total number of spatial data used are indicated numbers above the boxplots.

(B) (B) presents the average energy demand per climate zone (see also Table S4).

(C and D) In (C), the ratios of each climate zone to the entire terrestrial surface are shown, and in (D), their CDD and HDD shares are indicated. Climate zone E is not appropriate for establishing cleanrooms and thus has not been displayed. Climate data for the period 2021–2040 (Table S3) was used for the statistical analysis.

Impact correlation and parameter trade-offs (including future electricity mix, P4)

Through an examination of correlations between various parameters and results, we identified a significant trend in total energy consumption, Q_{total}, and its relation to the impact of 1 kWh of electricity consumption. The Pearson correlation coefficient (interval [−1,1]) for 2030 (P4) indicated a strong linkage between cleanroom indicator results across ISO 1 to ISO 9 (P1), climatic zone Q_{total} for each region (P2), and the impact of 1 kWh of electricity (medium voltage). A value closer to one in the correlation coefficient suggested a stronger linear correlation, whereas a value of −1 indicated an inverse correlation. This correlation was especially pronounced in higher ISO classes (ISO 1–5) where a higher cleanliness standard necessitates increased electricity usage, as shown in the data from the red rectangle in Figure 5A, which illustrated the impact of electricity usage and Q_{total} versus ISO classes. By contrast, the correlation was not as strong in lower ISO classes (ISO 6–9), where the relationship between electricity usage and ISO class began to decrease (ISO 8: 0.72, ISO 9: 0.54), while Q_{total} continued to rise, suggesting a larger impact of location-related factors, as supported by Figure 5B. To further clarify the relationship, Figure 5C depicts the percentage contributions of P1 and P2 to the overall impact against ISO classes. The heterogeneity in Figure 5C is attributable to the location of the cleanroom. It is possible that for more stringent ISO classes (such as ISO 1–5), the influence of P1 exceeds that of P2 in terms of percentage, as higher-class cleanrooms require more electricity for activities such as more frequent air change rates, resulting in a significantly higher percentage of electricity use than Q_{total} due to location and climatic zone. On the other hand, because electricity for operations in lower-rated ISOs is less expensive than in higher ones, an influence of P2 on the overall energy consumption begins to appear and its proportion begins to climb; Figure 5C illustrates this trend for ISO 6–9 in Q_{total}. At ISO 8, P1 and P2 both contribute approximately equally. As a result, there was no discernible correlation between climate zone and impact for ISO 1–5. Hence, we conclude that for cleanrooms with lower ISO classes, particularly ISO 6–9, geographic location or climate zone should be considered because the related Q_{total} would account for a greater proportion of total energy consumed.

Scenario studies of the influence of climatic zones on deciding on the installation of cleanroom facility

In reality, for practical purposes, several types of cleanrooms are utilized simultaneously in industrial applications. For example, semiconductor fabrication plants (commonly called "fabs") often employ a nested, modestly sized yet higher-class cleanroom inside a more massive but lower-class one to produce

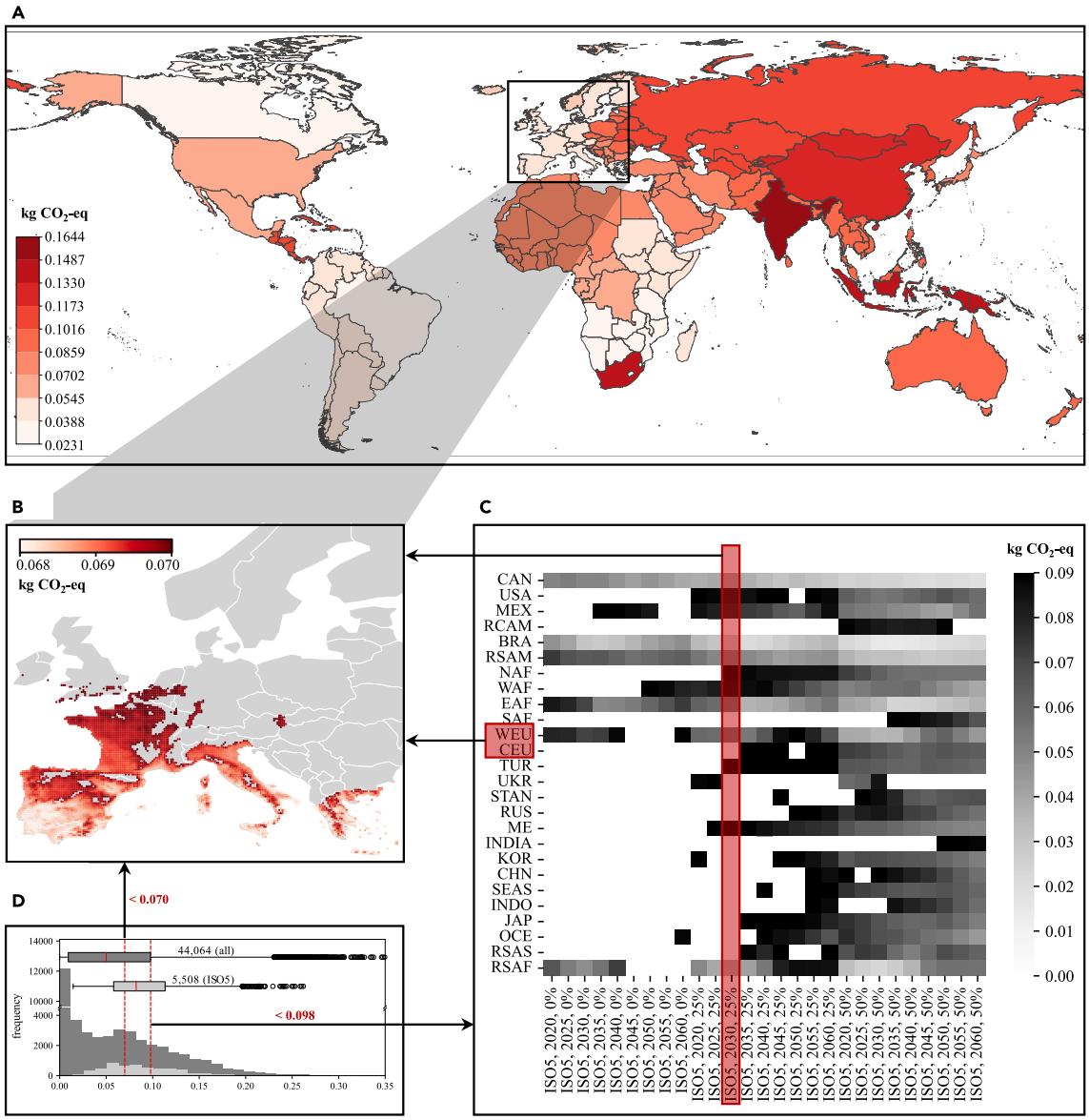

Figure 4. Example results of scenario impact screening for cleanrooms with ISO 5 and a 25% efficiency increase in 2030

(A) Indicator results (in kg CO_2-eq) of the impact category climate change using the midpoint method of the Intergovernmental Panel on Climate Change (IPCC, GWP 100a), aggregated by country.

(B) The same results were obtained for Europe (Western European Union [WEU] + CEU), which had a higher resolution and a threshold of 0.07 kg CO_2-eq (gray areas are beyond the threshold).

(C) An impact threshold of 0.098 kg CO_2-eq (75th percentile of all scenarios) was applied. White fields above the threshold have been filtered out.

(D) The impact indicator distribution of all (gray) data on the country level and for ISO 5 (light gray), with the thresholds indicated (red dashed lines).

wafers for chips. Previous studies showed that almost 40.4% of the total energy in a fab was consumed by process tools such as etching, film deposition, photolithography, and thermal diffusion/doping instrumentation, whereas the facility system accounted for 56.6% of the power.[48] Another study suggested that 30%–65% of the energy used in a high-tech fab was from the air-conditioning systems.[49] Because of the high construction, equipment expenses, and operating costs, large-scale use of high-quality cleanrooms may not always be financially possible or even necessary. In a fab, for example, a high-class (ISO 1–4) cleanroom, which may only be tens or hundreds of square meters in size, is often necessary for performing crucial process steps such as lithography and basic semiconductor processing areas. Other less significant phases, such as multi-layer processing and semiconductor wire-bonding and packaging service, could be conducted in a somewhat lower-standard cleanroom, such as ISO 5 or ISO 6, or a general service area in an ISO 8 cleanroom that may be hundreds or thousands of square

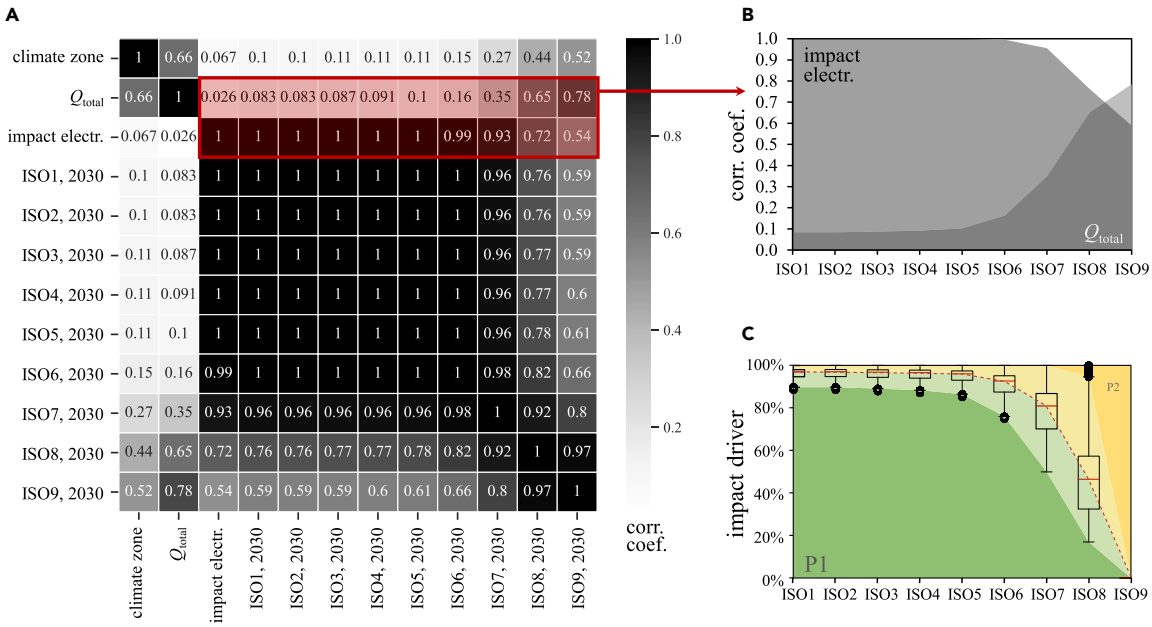

Figure 5. Correlation matrix and P1 and P2 as impact drivers

(A) For the year 2030 (P4), the Pearson correlation coefficient was calculated and is shown in (A).

(B and C) In (B), the correlation coefficient for the impact of electricity and energy demand for heating and cooling has been plotted against the ISO classes. The percentage contributions of P1 and P2 to the overall impact against ISO classes are shown in (C).

meters in size.[50] Therefore, the nesting of cleanrooms to varying degrees could drastically reduce total energy demand.

Scenario one

In this scenario, we simulated only a small portion of the production capacity to get a glimpse into the energy consumption of cleanrooms in a wafer fab. Let us consider, for illustration, that their reference year for the assessment is 2040 and that 25% of improvement takes place in the efficiency of the facilities in temperate zone. This scenario can be applied to describe the influence of climatic zones on electricity usage and Q_{total} more intuitively. In a medium-sized high-end chip-manufacturing plant, for example, a 50 m^2 high-class ISO 2 cleanroom was nested in a 550 m^2 ISO 4 one and then in a 1,400 m^2 ISO 5 space while they were designed to complete daily chip production in a 13,000 m^2 ISO 8 cleanroom, and the total area of the cleanroom is around 1/10 of fab 18 (160,000 m^2 cleanroom) of TSMC (the global leading semiconductor foundry). Based on the electricity usage of various ISO class cleanrooms presented in Table S1, the hourly electricity usage of each cleanroom and its share of overall electricity usage can be determined, as illustrated in Figure 6A.

From the results, we can find that the ISO 5 room accounts for 54% of overall electricity use. Based on the data in Table S2, the total energy requirement for such cleanrooms in various climate zones can be estimated. It was assumed that the total ISO electricity usage is the same in each climatic zone, whereas there was a significant variance for Q_{total}. The hourly Q_{total} needed for the cleanroom in that climate zone may be approximated given the known total area of the cleanroom. Figure 6B illustrates the percentage contribution of Q_{total} to the total energy consumption in various climate zones. It can be observed that in zone D (cold), not only was the total energy spent the largest, but Q_{total} also accounted for up to 45% of the total energy consumed. By contrast, zone C (temperate) has the lowest overall energy consumption, and its Q_{total} share was 23.4%, which could generate an energy savings of 22% compared with the cold zone. The Q_{total} proportioned in zone A (tropical) and zone B (arid) are 25.5% and 27.7%, respectively. Although the Q_{total} percentage difference between zone A (tropical), zone B (arid), and zone C (temperate) was not high in hours, this proportional discrepancy would result in a considerable disparity when calculating total yearly energy consumption, particularly if the cleanroom air exchange should continue during non-working hours. In this regard, it can be concluded that when employing lower-class cleanrooms in practical applications, the climate zone in which the cleanrooms were located could significantly influence the overall energy consumption owing to the large areas.

Scenario two

The second scenario was to validate our results about the IMAGE model obtained in different regions in the world (Figure S1 and repository file ISOall_pivot_region.xlsx). By applying the above cleanroom standards and scales to the IMAGE model-IMAGE_rfix 20 China (CHN), we can determine the equivalent CO_2 emissions for ISO 2, ISO 4, ISO 5, and ISO 8 cleanrooms in 2020. It was calculated that such cleanrooms located in the Taiwan region (CHN) would have an annual CO_2 emission (equivalent) of 5,352.01 tons. Meanwhile, we could obtain the equivalent CO_2 emissions by summing the electricity consumption of the ISO cleanrooms and the Q_{total} and then converting total electricity consumption into CO_2-eq by applying Taiwan's 2020

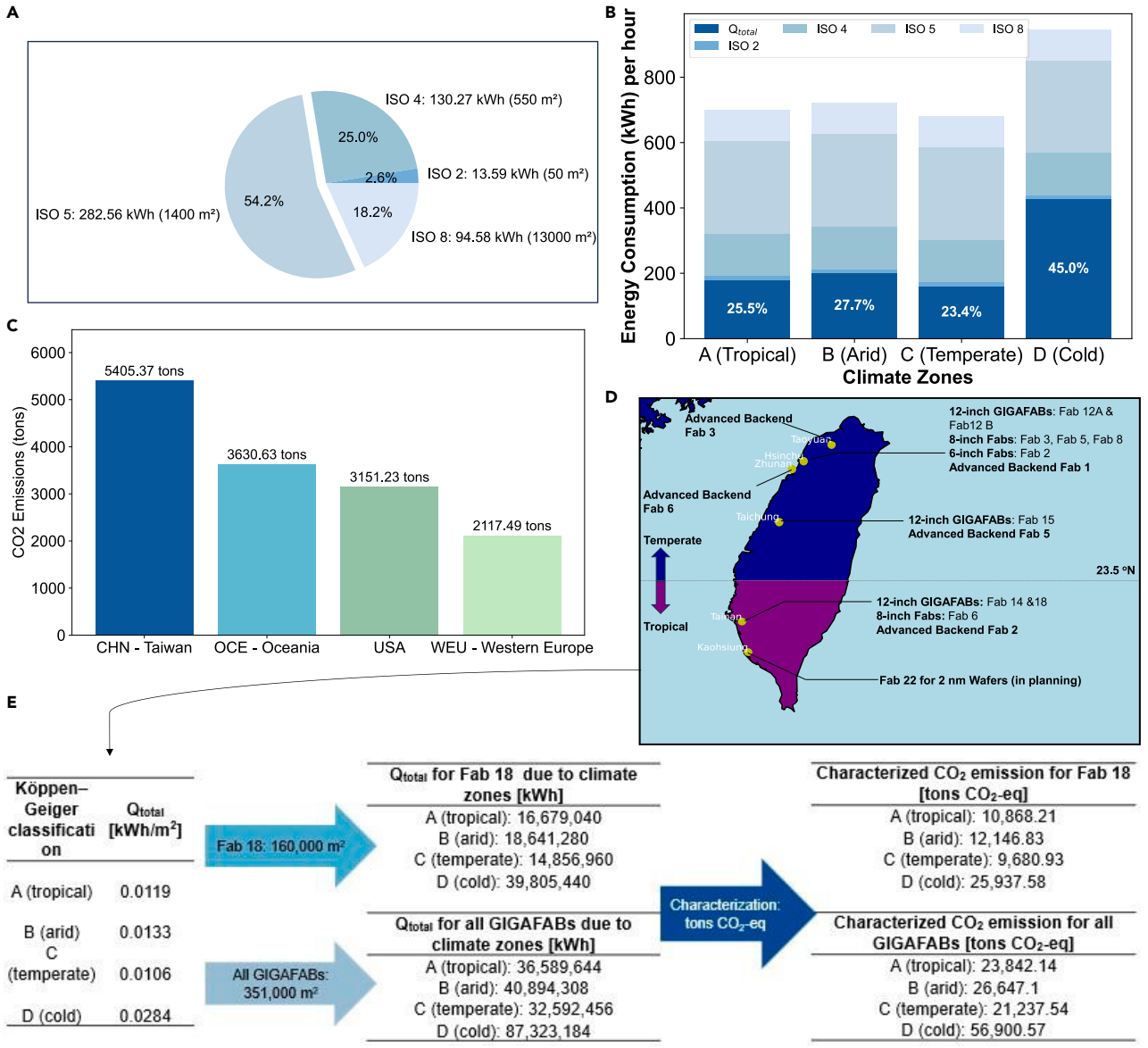

Figure 6. In a high-end chip-manufacturing plant scenario, there is a 50 m^2 high-class ISO 2 cleanroom nested within a 550 m^2 ISO 5 and 1,400 m^2 ISO 5 cleanroom, and they are implemented in a 13,000 m^2 ISO 8 cleanroom

(A) Hourly electricity usage of each ISO cleanroom and its portion of overall electricity usage.

(B) Percentage of Q_{total} relative to total energy consumption in different climate zones.

(C) Projected 2025 Cleanroom CO_2 emission using our model located in China (CHN), WEU, United States of America (USA), and Oceania (OCE).

(D and E) (D) A distribution map of TSMC wafer fabs in Taiwan on the left, including six located in the temperate zones of Hsinchu, Taichung, Taoyuan, and Zhu'nan, with the scale of each fab marked; and (E) the impact of climate zones on the Q_{total} of fab 18 and the effect of climate zones on the Q_{total} of all GIGAFAB® facilities, as well as their characterized CO_2 emission in tons.

electricity mix. According to the energy mix data, oil and petroleum products at 36.93% (730 g CO_2/kWh), coal at 33.06% (900 g CO_2/kWh), natural gas at 21.12% (400 g CO_2/kWh), and nuclear, solar, hydro, wind, and other renewable energies at a total of 8.88% (negligible CO_2 emissions).[51] The calculated characterized carbon emissions (tons CO_2-eq) amounted to 5,872.62 tons. This figure was close to the former calculation and thus corroborates the reliability of our research. Furthermore, projecting our study to 2025 and comparing the carbon emissions of cleanrooms of the same scale located in CHN, WEU, United States of America (USA), and Oceania (OCE), we found that the emissions numbers (tons CO_2-eq) were 5,405.37 tons, 2,117.49 tons, 3,151.23 tons, and 3,630.63 tons, respectively, as can be seen in Figure 6C. Our research can be further refined by considering that Taiwan spans both temperate and tropical zones, and more detailed studies in this

regard can lead to additional discoveries, thereby validating our research on the Q_{total} influenced by climatic zones.

Scenario three

Based on the 2022 annual report published by TSMC, the company had a value share of roughly 30% in worldwide semiconductor manufacturing throughout the year 2022.[52] Both in the first and second quarter of the year with over 50% market share of the global pure-play foundry market. During that particular year, TSMC and its subsidiaries successfully manufactured and processed a cumulative quantity of 15.3 million 12-inch equivalent wafers, which was a notable growth of 9% compared with the 14.2 million wafers processed in the preceding year of 2021.[52] Meanwhile, according to the data provided by the Energy Administration, Ministry of Economic Affairs of Taiwan, and TSMC's sustainability report, TSMC's electricity usage in the year 2022 amounted to about 8% of the total annual electricity consumption in Taiwan in 2022 and 14.3% of the whole industrial sector, and this number is almost half of the amount of the residential sector.[52,53] The main facilities as shown in Figure 6D, include four GIGAFAB® fabs (>100,000 pieces/month capacity for 300 mm [12″] wafers) with 12-inch wafers (fab 12, 14, 15,18), four fabs with 8-inch wafers (fab 3, 5 6, 8), and one fab with 6-inch wafers (fab 6) in Taiwan and other three overseas fabs (not shown).[52] As can be seen in Figure 6D, 8 fabs are located in the temperate zone (Hsinchu, Taichung, Taoyuan, and Zhu'nan) and 3 in Tainan.

Currently, TSMC's fab 18 is located in Tainan (a tropical zone [zone A]), with 160,000 m^2 of cleanrooms. According to our findings and calculation, the extra annual electricity consumption would be around 1.82 million kWh (1,187 tons of CO_2-eq, based on Taiwan's 2022 electricity mix) compared with that built in the temperate zone, as indicated in Figure 6E. Additionally, in Tainan, the cleanrooms of 8-inch fabs: fab 6 and advanced backend fab 2 were also affected by the climate zone. TSMC is planning to build a 2 nm wafer fab in Kaohsiung, which may lead to additional bulk electricity usage due to climate zone influences, but the extra power consumption cannot be estimated yet as the construction scale is currently unknown. Moreover, if we assume that a wafer fab similar to the TSMC fab 18 scale has its cleanrooms located in Arizona, USA (as TSMC is currently constructing new wafer fabs, known as the fab 21, in Arizona). Given Arizona's arid climate classification, the impact on Q_{total} would increase by 4.5%, resulting in an additional annual electricity consumption of 3.78 million kWh compared with that built in the temperate zone. However, the number for running it in a cold area will be 24.9 million kWh of extra electricity annually due to climate. If we further project that all the TSMC's GIGAFAB® scaled wafer fabs in 2022 were located in climate zones A, B, and D, respectively, the corresponding additional annual electricity consumption due to climate zones would be 4 (zone A), 8.3 (zone B), and 54.7 (zone D) million kWh, respectively, as demonstrated in Figure 6E. Correspondingly, the extra equivalent CO_2 emission would be 2,600, 5,400, and 35,600 tons, respectively. From the above studies, our research confirms that the choice of climate zone is significant when selecting a location for a wafer fab, considering extra energy consumption as well as carbon emissions due to climate zones.

Future cleanroom scenario carbon emission calculator

Based on the results of this study, we developed a future cleanroom scenario carbon emission calculator to assist users and decision-makers in estimating future scenario carbon emissions for cleanrooms in various climate zones. This calculator incorporates the four key parameters from this research, allowing the calculation of total emissions for different cleanroom levels. Users can input information for multiple countries or regions, including nested cleanrooms in different future scenarios. After entering the information, the calculator displays the results on a world map and generates a CSV file with total carbon emissions and nested cleanroom emissions for each country. The software is available in the data and code availability part.

DISCUSSION

To assess the environmental sustainability of cleanrooms under changing climate and energy scenarios, this study applied ex-ante LCA with specific alterations combined with the general morphology analysis (GMA) approach so that it is convenient to parameterize the intricate problem of cleanroom energy consumption and evaluate it in conjunction with a climate change model. Four parameters were identified: *electricity per ISO standard* (P1), *electricity per climate zone* (P2), *technology efficiency increase* (P3), and *future electricity mix* (P4). Based on these defined parameters, there were nine different ISO standards for cleanrooms, three different technical efficiency options, nine future electricity mixes, and 529,539 spatial geo-data points, which could be averaged, for example, per country (204 countries). This combination led to over 68 trillion different impact indicator results or 49,572 results at the country level, and 243 impact indicator maps were generated using our approach. To screen complex cleanroom scenarios and determine their environmental impacts, we modeled future scenarios, spatial-temporal data, climate, and electricity mixes. Furthermore, we concentrated on locating important characteristics and exploring and screening a sizable scenario space.

As for energy demand per climate zone (P2), according to Isaac and van Vuuren,[54] there has been a 70% increase in the demand for cooling energy, particularly in developing countries, since the beginning of the twenty-first century; this effect may be attributed to increased prosperity in those countries as well as to global climate change. By contrast, these authors also discovered that the global demand for heating energy has decreased by approximately 30%. This observation may imply that tropical and arid regions may require more energy for cooling whereas areas with low temperatures may require less energy for heating overall; however, there was no discernible trend in Q_{total} and Köppen-Geiger classification except in zone E (polar areas; Figure 3A, yellow), which is not primarily appropriate for cleanroom locations and thus not discussed in this study. Temperate locations require the lowest value of Q_{total}, 0.0106 ± 0.0040 kWh/m^2, as shown in Figure 3B and Table S4, making the cleanrooms in this zone the most energy efficient. Building a cleanroom in the cold zone, on the other hand, is the least favorable in terms of energy consumption, because it requires the highest overall energy consumption Q_{total}, 0.0284 ± 0.0081 kWh/m^2. When comparing higher-class cleanrooms, such as ISO 5 to ISO 1, the impact of

P2 Q_{total} is only approximately 3%–10% of P1 ISO class electricity use (with ISO class electricity use ranging from 0.2691 to 0.3625 kWh/m^2, according to Table S2). As a result, when constructing predominantly high-ISO class cleanrooms, the cleanroom's location does not seem to make a major impact.

In addition, radiative forcing targets primarily affect temperature, making bringing the representative concentration pathway (RCP) component to an equivalent scenario even more important. When the global mean temperature (IMAGE model) of various shared socioeconomic pathway (SSP)-RCP combinations were compared, the SSP3–7.0 (climate data) and SSP2–6.0 (energy data) behaved almost equally until 2060 (data not shown). However, local variations might arise and introduce uncertainty into the overall approach. Nevertheless, the combination of SSP3–7.0 for the climate data and SSP2–6.0 for the LCI energy data seemed to provide the best fit and, therefore, was used in this study. Both RCP6.0 and RCP7.0 represent scenarios in which no or very little further effort has been made to constrain emissions, making a global temperature increase above 3°C very likely.[55,56]

Limitations and outlook

In this research, we showed that the location of cleanrooms is important under certain technological and climatic conditions, particularly when using cleanrooms with very large areas as demonstrated by our example, in which approximately 22% of energy could be saved if the location of cleanrooms is to be selected appropriately. We have further validated our findings using the Q_{total} of TSMC fabs cleanrooms as an example to emphasize the importance of selecting climate zone installation locations. In addition to cleanrooms, users of other energy-intensive systems that may be affected by location as well as current and future climatic conditions could apply the method developed in this study to generate scenarios and energy consumption estimates. Regarding climate change in other cases, readers may also refer to Figure S1.

Some limitations and potential modifications exist regarding future work. For example, one of the uncertainties that this study did not address is electricity consumption by other equipment in cleanrooms of higher ISO classes. Heating, ventilation, and air-conditioning (HVAC) systems are a significant source of energy consumption in high-tech fabrication facilities, comprising 30%–65% of the total energy use. The uncertainty in HVAC end-form and control methods can indeed influence the results.[28,57,58] For example, certain HVAC systems in semiconductor cleanrooms maintain precise humidity at such low levels that extra instruments, such as air ionizers, are necessary to defend against electrostatic discharge and avoid damage to the circuit designs.[58] In addition, cleanroom operation processes also generate additional loads. In future studies, decomposing the heating and cooling energy consumption, such as internal load, load through the envelope, and load through ventilation, could help better understand the direct impact of climate conditions on these loads.[27,59]

Furthermore, integrating proper air distribution strategies, effective filtration, and accommodating user-induced disturbances are also crucial for optimizing cleanroom energy consumption and operational efficiency.[8,25,26] For example, considering occupant movements and other disturbances is essential, as human interactions can introduce turbulence, influence particle dispersion, and disrupt airflow patterns, decreasing the efficiency of contamination control measures.[25] These factors should be included in future research.

Material flows have also been omitted thus far but may include materials from construction, filter maintenance, and other sources. Despite the generic cleanrooms covered in this study, different types of cleanrooms with varying needs from various industrial domains, such as biological laboratories, good manufacturing practice (GMP) cleanrooms for pharmaceuticals, and cleanrooms for fabs, among others, may be studied in more depth; the abovementioned contents are often related to P1. Thus, the morphospace, or technical parameter space (gray boxes in Figure 7), may also be refined and modeled if necessary. For example, the total make-up air unit (MAU) and the recirculation air unit (RC) consist of different coils, including a mixing section and different fan units of the air handling unit (AHU, Figure 8). As the MAU pre-processes the air from outside the cleanroom, the RC and AHU condition the recirculated air.[60] This system can also be precisely modeled to investigate the energy contribution of each subunit under various conditions.[45,60] In addition, other studies have found that the design and control of cleanroom air-conditioning systems can reduce the heating and cooling energy demand by 87.8% and 69.6%, respectively.[61] Thus, other HVAC devices, such as MAU + AHU + high-efficiency particulate absorbing filter (HEPA) or MAU + dry cooling coil (DCC) + fan filter unit (FFU) systems, could also be studied to modify the parameters in this work.

Although almost identical results until 2060 were derived using SSP3–7.0 (climate data) and SSP2–6.0 (energy data) for the global mean temperature (IMAGE model), the mismatch of climate data for tier 1 SSP-RCP combinations with LCA inventory data for future electricity mixes for other SSP-RCP combinations could pose uncertainties and challenges to more precise analysis of these characteristics. Therefore, the resolution of this issue could assist in reducing the uncertainty of scenarios. Moreover, this research only applied the one-letter level of climate zones, whereas it could be further modified if sub-zones were to be considered.[62] Other factors, as listed in Figure 8, can also be studied, such as local air quality. Given that outside air is employed in the air intake procedure during the air circulation step, excessive particulate matter requires additional energy to treat, in addition to the relatively high necessity for air filtration devices. Thus, air pollution or the quality of the air in cleanroom sites is a concern that may need to be addressed in future research. However, due to the complexity of the LCI parameter solutions space (P1–P4), only a few AHU characteristics were considered in this work. Suggested future work might include issues such as adaptation to air pollution or gaseous chemical contaminants and other LCI problems or integration into scenario development. Moreover, future studies regarding electricity mixes in cleanroom operations should consider integrating renewable energy sources to reduce carbon emissions.

EXPERIMENTAL PROCEDURES

LCA and sustainability profile of cleanrooms

LCA is the most advanced method available to identify the environmental burdens of a product system and to guide policymakers and proactive companies

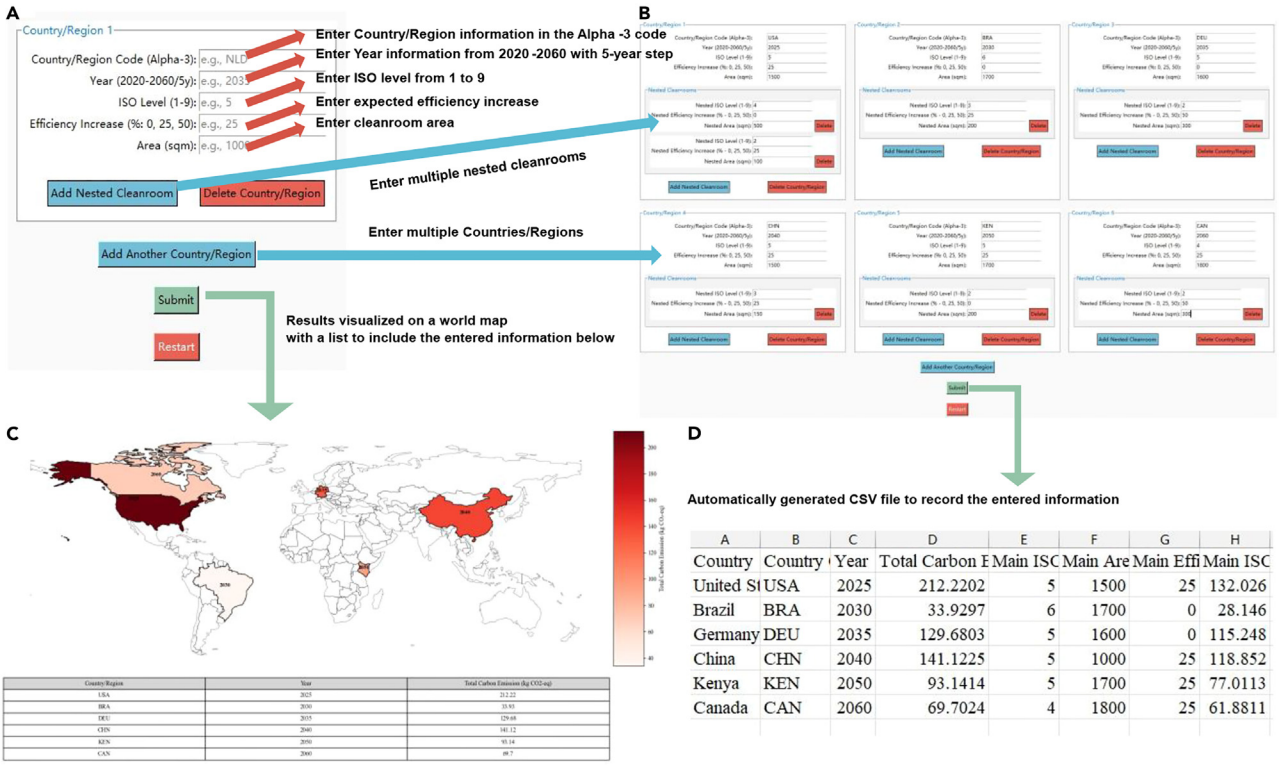

A	B	C	D	E	F	G	H
Country	Country	Year	Total Carbon E	Main ISC	Main Are	Main Effi	Main ISC
United St	USA	2025	212.2202	5	1500	25	132.026
Brazil	BRA	2030	33.9297	6	1700	0	28.146
Germany	DEU	2035	129.6803	5	1600	0	115.248
China	CHN	2040	141.1225	5	1000	25	118.852
Kenya	KEN	2050	93.1414	5	1700	25	77.0113
Canada	CAN	2060	69.7024	4	1800	25	61.8811

Figure 7. Cleanroom future scenario energy consumption calculator

(A) User interface.

(B) Multiple entry of country and nested cleanroom.

(C) Results display on a world map with a list.

(D) Automatically generated CSV file to record the entered information.

to make well-informed sustainability decisions.[30,63,64] The fundamental drive toward sustainable technology production and their frequent reliance on cleanrooms make LCA an optimal tool for assessing the environmental impact of these facilities.[34,65] The use of cleanrooms is not new, and some LCA studies have incorporated their usage; however, the available LCI data for this service of a clean space usually is outdated, scarce, and very inconsistent depending on many factors. This is due to several influencing factors. Primarily, thanks to technological advancements in the rapid expansion of micro-nanofabrication technology, cleanrooms evolved remarkably in design and operation, rendering older data obsolete.[66] Moreover, variations in operational protocols, equipment types, and maintenance practices across different facilities contribute to inconsistencies in the data.[67] Additionally, geographic and climatic differences also play a role in the variability of energy use and material requirements.[27] For this study, we collected LCI data from the ecoinvent database[68] regarding the electricity information of different countries or regions and relevant literature on GHG emissions for relevant processes in the cleanroom value chain and characterized their impacts on climate change using the characterization factor of GWP.[43–45] Here, we followed the recommended methodology of the IPCC (GWP 100a: weighted sum of the amount of GHGs emitted by the system in kg CO_2-eq).[55,56] We performed all calculations using LCA Activity Browser software.[69]

GMA

To overcome some of the challenges of standard LCA approaches and model a complex cleanroom system, we combined LCA with GMA.[70] GMA allows the investigation of the totality of relationships present in multi-dimensional complex systems, including those with non-quantifiable characteristics.[70] In this context, a parameter is one of a set of factors that defines a system and determines its behavior and must not be part of a mathematical function per se.[71] Relevant parameters are connected in a normative, logical, causal, and statistical fashion in GMA. The fundamental framework of a GMA model is, therefore, internally connected by its parameters, resulting in an *n*-dimensional conceptual space known as a morphospace.[71] Each parameter head or variable (e.g., cleanroom-dependent products) usually consists of several parameters or value ranges (e.g., pharmaceutical products, integrated circuits, semiconductors, or solar panels). After defining all relevant parameters with their ranges, GMA proposes a cross-consistency assessment (CCA) to narrow the total set of possible configurations in the morphospace and finally develop and assess the possible resulting scenarios.[72]

Based on its broad applicability, GMA has been employed in several research fields and has even been applied in political decision-making.[73–75] In LCA, it has been applied, among other approaches, to define future scenarios or to address non-quantifiable uncertainties.[55,56] While future scenarios have often staked out the extremes of a solution space (e.g., worst case, best case, and black swan events), our study has accounted for a vast number of other situations and scenarios. Such an extensive exploration of scenarios allows for assessing cleanrooms per their requirements (specific locations, cleanroom ISO standards, etc.) and evaluating potential trade-offs among parameters and whether certain regions would constitute more sustainable future cleanroom locations.

Identification of relevant parameters to model cleanrooms

Estimating how much energy a cleanroom consumes is challenging, as the overall energy consumption required to maintain a specific ISO standard depends on several parameters (e.g., the technical equipment used or the number of people concurrently working in the facility). Xu and Tschudi[43] examined

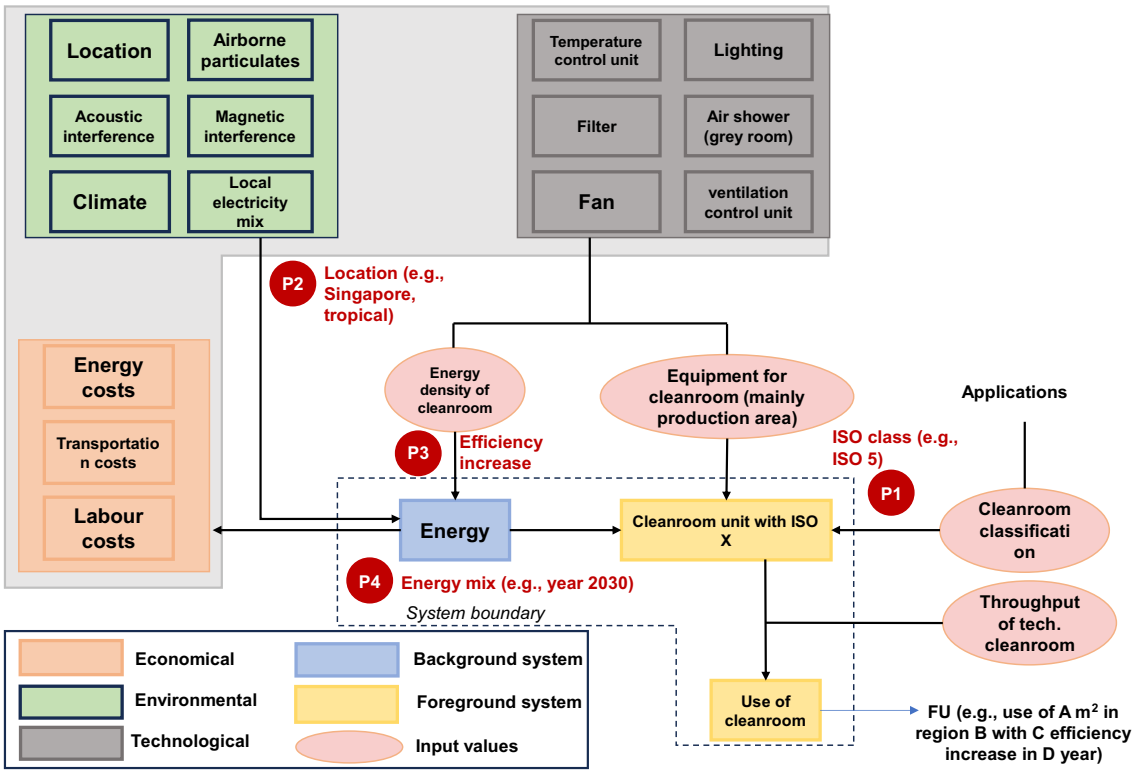

Figure 8. Flow chart of the general cleanroom parameters that can be linked to the LCI

The parameters have been divided into three morphospaces: economical parameters (orange), environmental parameters (green), and technical parameters (gray). The system boundary is in a dashed box. Direct LCI parameters are indicated by a light blue background and external parameters by a light gray background. LCI-relevant input values for cleanrooms are highlighted in red ovals, and foreground and background unit processes are in blue and yellow, respectively. For the sake of clarity, not all relationships (indicated by arrows) between the parameters are shown. In this context, environmental parameters are parameters that are influenced by their location and surroundings. A parameter combination example of a cleanroom scenario (P1–P4) is provided in red.

the energy performance of 13 cleanrooms with different recirculation systems. Five of them fell into the category of ISO class 4, seven into category 5, and one into class 5/6. Williams et al.[44] provided experimental energy and air exchange rate data for ISO 3, ISO 4, and ISO 5, and Ludlage et al.[45] provided data for one experimental value for ISO 7. Based on the works mentioned above, we extrapolated the energy demand for the remaining ISO classes by following the cleanroom recommendations of IEST-RP-CC012.1[42] for air changes per hour and airflow rates.

We focused on the operation of cleanrooms and set the system boundary of our study to include the energy to power the cleanrooms, the specific ISO standards defining the cleanroom setup, and the use of cleanrooms, as shown in the dashed box on the bottom right in Figure 8. In relation to the operation of cleanrooms, we assessed four key influencing factors (Figure 8, red ovals):

(1) The cleanroom classification required (and currently in use).
(2) The energy density of the cleanroom configuration (kWh/m^2).
(3) An extrapolation of the equipment needed (i.e., the area that is occupied to produce the device or the production area in m^2; here, the devices can also be technical devices or others such as chips, etc.).
(4) The throughput (by devices per hour).

We translated the factors above into modeling constructs and linked them in software to LCI data, as follows (see also Figure 8). To this end, we identified and categorized cleanrooms using technological, economic, and environmental parameter spaces (Figure 8, gray, orange, and green boxes, respectively) in line with the GMA approach previously described. In this context, technological parameters consider all the factors varying with the ISO standards that are applied for each cleanroom class and their energy demand in use. These factors and standards determine the mode of operation of cleanrooms and the related technical specifications (e.g., the ability to control particles with different sizes).[15] All such factors were determined in our later calculations of the *electricity per ISO standard*, P1 (Figure 8, P1). Furthermore, we considered how the local climatic conditions of operation can influence the performance of cleanrooms. In turn, the location affects the amount of energy needed to reach a certain level of air purity. Such considerations were included in the models as *electricity per climate zone*, P2 (Figure 8, P2), Here, we modeled the energy demand for ensuring a constant temperature (energy for cooling and heating) of cleanrooms in specific climate zones, considering the electricity mix for each location across the extent of the Earth. Moreover, we considered an incremental improvement over time in the efficiency of cleanroom technology and its management, and we translated such an increase using the *technical efficiency increase*, P3 (Figure 8, P3). In our models, we also quantified the influence of the evolution of the energy system over time and implemented that using the factor *future electricity mix*, P4 (Figure 8 P4).

For all the subsequent calculations and scenarios, we defined the functional unit (FU in Figure 8) as the energy needed to operate 1 m^2 of a cleanroom under ISO standard A (P1, range 1–9) installed in region B (P2, region of choice) with C efficiency increment (P3, 0%–50%) in the time period D (P4, range 2020–2060) to produce one technical device per hour. The FU is the basis of all comparative assessments in LCA.[30] For the example in Figure 8 (in red), this FU would be defined as the energy needed to operate 1 m^2 of cleanroom under ISO standard 5 conditions in Singapore in 2030 to produce one technical device per hour.

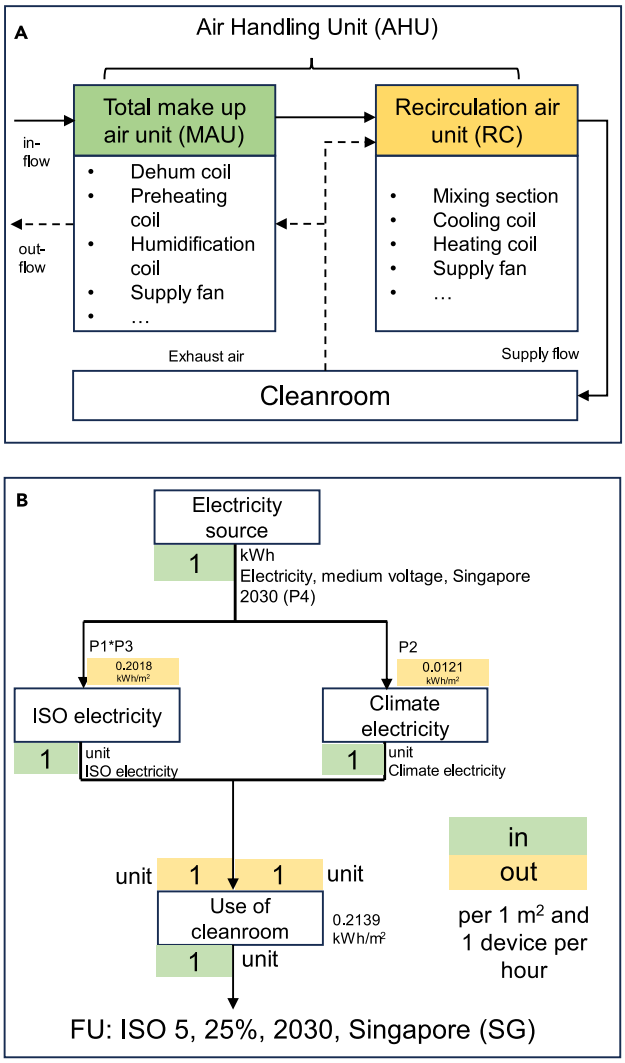

Figure 9. Characterization of the cleanroom

(A) Schematic drawing of individual components that can affect the conditions of the air handling unit of cleanrooms.[60]

(B) Illustration of the total electricity usage of a cleanroom as modeled in this study, using Singapore as an example.

Figure 9A depicts the AHU, which is the key working unit for treating incoming air. The AHU includes the two most important units, which are the MAU and the RC, as well as their key components. In this research, changes in the surrounding temperature were considered in P3 (part of the MAU), and the electricity usage to ensure a certain ISO standard was considered in P1 (mainly associated with the RC unit). The findings of Ludlage et al.[45] in reducing the air exchange rate of the cleanroom outside operating hours were integrated into P3 as a potential improvement in efficiency. Of course, other strategies (such as airflow optimization, solar pre-heating, heat recovery system, improved lighting controls,[28,76] etc.) may be used to obtain higher efficiencies, but the findings of Ludlage et al.[45] indicated that there is room for improvement in terms of reducing the energy requirements of cleanrooms. Based on this publication, three efficiency states for P3 were chosen: 0% (status quo), 25% (medium optimization), and 50% (high optimization). Figure 9B shows how the parameters work using Singapore as an example. The total energy consumption is a sum of the ISO electricity usage and energy consumption due to the climate zone. The efficiency increase was applied to the ISO electricity usage part. Furthermore, it is to be noted that material flows were negligible in this study when compared with the major contributor, which was energy.

Definition of scenarios and connection to LCI data

To assess the climate change impacts of cleanroom scenarios, we developed a computational pipeline that maps cleanroom characteristics to various solution spaces and connects them to LCI data in the supplemental information.

We identified four key LCI-linked parameters—P1 (electricity per ISO standard), P2 (electricity per climate zone and country), P3 (technical efficiency increase), and P4 (future electricity mix)—and assessed their permutations to determine the environmental impacts of each scenario (see Figure 10 for a section of the scenario space). We estimated the electricity consumption of cleanrooms in different countries by multiplying the parameters P1 to P4. The total electricity consumption includes ISO electricity usage and climatic zone electricity consumption, both of which are influenced by technology efficiency increases. For each scenario S, a corresponding impact score (IS) was calculated. Based on the four LCI-linked parameters, we evaluated 50,000 scenarios of cleanroom operations and quantified their climate change impacts. This resulted in 68 trillion IS, representing the climate change impacts of cleanrooms potentially located on any 5-km^2 spatial cell within the entire extent of the Earth.[56,77,78] Using Singapore as an example, we estimated that an ISO 5 cleanroom with a 25% efficiency improvement in 2030 would consume 0.214 kWh/m^2 of electricity, as demonstrated in Figure 9B. Moreover, to make the results more useful and accessible, we developed a cleanroom energy consumption calculator for future scenarios based on these results. The software can be found from the link in the data and code availability part.

Future scenarios for spatial and temporal climate data and electricity mixes

We used SSPs[79] to address the future evolution of cleanrooms in consistent scenarios. SSPs define five possible pathways (SSP1–5) as global consensus scenarios regarding how global society, demographics, and economics may evolve over the next century.[79] SSPs map the future socioeconomic dependencies of the world's RCPs that are focused solely on climate futures that depend on the amount of GHGs emitted.[80] The IPCC produced the fifth assessment report (AR5)[55] in 2014 by integrating the SSPs into a combined SSP-RCP framework (AR6, IPCC).[56] O'Neil et al.[81] mapped all conceivable combinations in their coupled model intercomparison project (CMIP6), reflected on their prioritization, and eventually proposed two tiers. Tier 1 serves as the basis for climate model projections with the following SSP-RCP combinations: SSP1–2.6, SSP2–4.5, SSP3–7.0, and SSP5–8.5; the latter number represents the radiative forcing value (e.g., 2.6 W/m^2) in 2100. The second tier includes additional scenarios to address policy discussions of mitigation pathways.[81] In theory, 5 × 7 SSP-RCP combinations are possible. For an interpretation of the SSP-RCP concepts and other parameters mentioned in this subsection, please refer to the supplemental information section further explanations part.

We used climate data available for the tier 1 SSP-RCP combination and considered the most relevant combinations and LCI data available for future electricity mixes. Spatiotemporal data were required to account for future electricity mixes (P4) and the energy demand per climate zone (P2) in the cleanroom scenarios. The data listed in Table S2 were used for parameters P2 and P4. We retrieved the spatiotemporal climate data for the proposed tier 1 climate model projections from WorldClim,[78] O'Neill et al.,[81] and the sixth assessment report (AR6) of the IPCC.[56] We applied the lowest resolution, 10 arc min, to acquire global results in an adequate simulation time; however, it would also be feasible to raise the resolution for certain regions if more detailed investigations were to be required. For the SSP3–7.0 future scenario, the medians of nine general circulation models (GCMs, WorldClim)[78] were averaged in our calculation for the time periods 2021–2040 and 2041–2060. For the historical (1980–2016) and future (2071–2100) periods, the Köppen-Geiger climate classification was employed for calculation as well, and this classification is available for RCP8.5.[47] For climate zone data, we used the main climate zones according to the relevant climate classification. The background energy data of the LCI database ecoinvent was updated via the superstructure

		S1	S2	S3	S4	S5	S6	S7	S8	S9	S10	…	S149572
Electricity per ISO standard	ISO1	X									X	…	
	ISO2		X									…	
	ISO3			X								…	
	ISO4				X							…	
	ISO5					X						…	
	ISO6						X					…	
	ISO7							X				…	
	ISO8								X			…	
	ISO9									X		…	X
Electricity per climate zone & country	AD (C)	X	X	X	X	X	X	X	X	X		…	
	AE (B)										X	…	
	⋮	⋮	⋮	⋮	⋮	⋮	⋮	⋮	⋮	⋮	⋮	…	⋮
	ZW (B)											…	X
Tech efficiency increase	0%	X	X	X	X	X	X	X	X	X	X	…	
	25%											…	
	50%											…	X
Future electricity mix	2020	X	X	X	X	X	X	X	X	X	X	…	
	2025											…	
	2030											…	
	2035											…	
	2040											…	
	2045											…	
	2050											…	
	2055											…	
	2060											…	X
Impact score (IS)		IS1	IS2	IS3	IS4	IS5	IS6	IS7	IS8	IS9	IS10	…	IS49572

Figure 10. Mapping of possible scenarios

The LCI morphospace has four parameter ranges: electricity per ISO standard (P1), 9 scenarios; electricity per climate zone and on the country level here (P2), 204 scenarios; technical efficiency increase (P3), 3 scenarios; and future electricity mix (P4), 9 scenarios. The total number of possible scenarios on country resolution is P1(9) × P2(204) × P3(3) × P4(9) = S (49,572). Each scenario (S) has a corresponding impact score (IS).

approach and was linked to the IMAGE model.[68,77,82–84] Future electricity mixes are available for 26 regions (Figure S1 and SSP-RCP combination SSP2–6.0, sometimes referred to as SSP2-base) in 5-year increments for 2020–2060.

Deriving energy demand per climate zone via HDD/CDD correlation

We used a common method of determining the energy demand for temperature control in a room, i.e., the evaluation of HDD and CDD.[46] We derived heating and cooling days over time and with changing climate using the daily local mean temperature, which can be calculated using the spatial-temporal climate data mentioned above. The energy demand for maintaining a certain temperature in a room correlates with the ambient (outdoor) temperature, expressible in HDD and CDD. To convert the local HDDs and CDDs, the reference temperature of 18°C was chosen. We estimated the heating and cooling energy demands via the correlation proposed by De Rosa et al.[46]

Degree days (DDs) are defined as the sum of the positive differences between the reference temperature T_{ref} and the daily average outdoor temperature T, which are usually accumulated per year and expressed in °C.[85,86] For the spatiotemporal outdoor temperature, the mean of the monthly average minimum and maximum temperature $T_{min/max}$ was taken. To derive the HDDs, the outdoor temperature is subtracted by the reference temperature when $T \leq T_{ref}$:

$$HDD = T_{ref} - T$$

$$CDD = 0 \qquad \text{(Equation 1)}$$

Conversely, in the case of CDDs, the differences are calculated only when $T \geq T_{ref}$:

$$CDD = T - T_{ref}$$

$$HDD = 0 \qquad \text{(Equation 2)}$$

All final parameters for the life cycle impact assessment (LCIA) calculations, screening method, simulation tools, and literature sources are summarized in Table S5. The climate data were pre-processed in R, and we used the LCA Activity Browser[69] software to calculate the indicator results (in kg CO_2-eq) of the impact category climate change by using the midpoint method of the IPCC, GWP 100a for each IMAGE region (1 kWh electricity, background unit process: market group for electricity, high voltage) and considering a specific reference year. The final cleanroom scenario combinations of P1–P4 were performed using Python.

RESOURCE AVAILABILITY

Lead contact

Any requests for further information should be directed to Stefano Cucurachi (s.cucurachi@cml.leidenuniv.nl).

Materials availability

This study generated a future cleanroom scenario carbon emission calculator, which can be found at https://surfdrive.surf.nl/files/index.php/s/c1mtFlPXhr828Bt. The folder is named Cleanroom Future Scenario Carbon Emission Calculator.

Data and code availability

The datasets generated and/or analyzed during this study are available in the supplemental information at: https://surfdrive.surf.nl/files/index.php/s/c1mtFlPXhr828Bt.

The folder is named Data for Environmental Sustainability Assessment of Cleanrooms under Changing Climate and Energy Scenarios.

ACKNOWLEDGMENTS

The authors are very grateful to Sebastiaan Deetman from Leiden University for his support and guidance during data collection for SSP scenarios. We would also like to express our gratitude to Marcel G.L.C. Loomans from TU Eindhoven for sharing his extensive knowledge of building performance and cleanrooms and for providing valuable feedback regarding our research. This work was funded by the European Union's Horizon 2020 Research and Innovation Program within the project PROGENY (grant number 899205). PROGENY is coordinated by Technische Universität Dresden and managed by Wasabi Innovations Ltd.

AUTHOR CONTRIBUTIONS

Literature collection, J.Z.L. and F.S.; methodology, J.Z.L., F.S., and S.C.; coding, J.Z.L. and F.S.; software, J.Z.L.; writing – original draft, J.Z.L.; conceptualization, F.S. and S.C.; writing – review and editing, F.S., B.R.P.S., A.J., V.B., R.W., K.L., I.S., and S.C.

DECLARATION OF INTERESTS

The authors declare that they have no known competing financial interests or personal relationships that could have appeared to influence the work reported in this paper.

SUPPLEMENTAL INFORMATION

Supplemental information can be found online at https://doi.org/10.1016/j.crsus.2024.100219.

Received: February 23, 2024
Revised: August 10, 2024
Accepted: August 27, 2024
Published: September 19, 2024

REFERENCES

1. Mohammad, W., Elomri, A., and Kerbache, L. (2022). The global semiconductor chip shortage: causes, implications, and potential remedies. IFAC PapersOnLine *55*, 476–483. https://doi.org/10.1016/j.ifacol.2022.09.439.
2. Ruberti, M. (2023). The chip manufacturing industry: environmental impacts and eco-efficiency analysis. Sci. Total Environ. *858*, 159873. https://doi.org/10.1016/j.scitotenv.2022.159873.
3. Estreicher, S.K., Backlund, D., and Gibbons, T.M. (2009). Non-equilibrium dynamics for impurities in semiconductors. Phys. B *404*, 4337–4340. https://doi.org/10.1016/j.physb.2009.09.024.
4. Gopinath, S.C.B., Ramanathan, S., Mohd Yasin, M.N., Shapiai Razak, M.I., Ismail, Z.H., Salleh, S., Sauli, Z., Malarvili, M.B., and Subramaniam, S. (2022). Failure analysis on silicon semiconductor device materials: optical and high-resolution microscopic assessments. J. Mater. Res. Technol. *21*, 3451–3461. https://doi.org/10.1016/j.jmrt.2022.10.116.
5. Whyte, W. (2010). Cleanroom Technology: Fundamentals of Design, Testing and Operation (John Wiley & Sons).
6. Yin, J., Liu, X., Guan, B., and Zhang, T. (2020). Performance and improvement of cleanroom environment control system related to cold-heat offset in clean semiconductor fabs. Energy Build. *224*, 110294. https://doi.org/10.1016/j.enbuild.2020.110294.
7. Jo, M.-S., Shin, J.-H., Kim, W.-J., and Jeong, J.-W. (2017). Energy-saving benefits of adiabatic humidification in the air conditioning systems of semiconductor cleanrooms. Energies *10*, 1774. https://doi.org/10.3390/en10111774.
8. Bhattacharya, A., Metcalf, A.R., Nafchi, A.M., and Mousavi, E.S. (2021). Particle dispersion in a cleanroom – effects of pressurization, door opening and traffic flow. Build. Res. Inf. *49*, 294–307. https://doi.org/10.1080/09613218.2020.1720500.
9. Zhang, F., Shiue, A., Fan, Y., Liu, J., Meng, H., Zhang, J., and Leggett, G. (2022). Dynamic emission rates of human activity in biological cleanrooms. Build. Environ. *226*, 109777. https://doi.org/10.1016/j.buildenv.2022.109777.
10. Sofia Paulino Mendes, A., Rutgersson, A., and Paulsson, M. (2022). Outdoor environmental effects on cleanrooms – A study from a Swedish hospital pharmacy compounding unit. Eur. J. Pharm. Biopharm. *177*, 100–106. https://doi.org/10.1016/j.ejpb.2022.06.003.
11. Wang, C., Holmberg, S., and Sadrizadeh, S. (2018). Numerical study of temperature-controlled airflow in comparison with turbulent mixing and laminar airflow for operating room ventilation. Build. Environ. *144*, 45–56. https://doi.org/10.1016/j.buildenv.2018.08.010.
12. Dotter, M., Storck, J.L., Surjawidjaja, M., Adabra, S., and Grothe, T. (2021). Investigation of the long-term stability of different polymers and their blends with PEO to produce gel polymer electrolytes for non-toxic dye-sensitized solar cells. Appl. Sci. *11*, 5834. https://doi.org/10.3390/app11135834.
13. Sutherland, K. (2008). Cleanroom management: using filters in the cleanroom. Filtr. Sep. *45*, 20–22. https://doi.org/10.1016/S0015-1882(08)70088-0.
14. Pasanen, T.P., von Gastrow, G., Heikkinen, I.T.S., Vähänissi, V., Savin, H., and Pearce, J.M. (2019). Compatibility of 3-D printed devices in cleanroom environments for semiconductor processing. Mater. Sci. Semicond. Process. *89*, 59–67. https://doi.org/10.1016/j.mssp.2018.08.027.
15. ISO-14644-1 (1999). Cleanrooms and Associated Controlled Environments. Part 1: Classification of Air Cleanliness. ISO Standard 14644-1 (The Institute of Environmental Sciences and Technology (IEST)).
16. Lin, T., Tung, Y.-C., Hu, S.-C., and Chen, Y.-J. (2011). Experimental study on airflow characteristics and temperature distribution in non-unidirectional cleanrooms for electronic industry. Build. Environ. *46*, 1235–1242. https://doi.org/10.1016/j.buildenv.2010.10.028.
17. Mičko, P., Hečko, D., Kapjor, A., Nosek, R., Kolková, Z., Hrabovský, P., and Kantová, N.Č. (2022). Impact of the speed of airflow in a cleanroom on the degree of air pollution. Appl. Sci. *12*, 2466. https://doi.org/10.3390/app12052466.
18. Shao, X., Hao, Y., Liang, S., Wang, H., Liu, Y., and Li, X. (2022). Experimental characterization of particle distribution during the process of reducing the air supply volume in an electronic industry cleanroom. J. Build. Eng. *45*, 103594. https://doi.org/10.1016/j.jobe.2021.103594.
19. Maeda, M., Toshihito, T., and Akira, T. (1986). Studies on rationalizing air flow in clean room (Part 1): Air flow pattern in a vertical laminar flow type clean room. In Proceedings of the 5th Annual Technical Meeting of Japan Air Cleaning Association, Tokyo, Japan, pp. 115–122.
20. Takahashi, A., and Okada, T. (1990). Configuration of vertical laminar flow (VLF) type cleanrooms and non-uniformity in airflow profile. In Proceedings of the 10th International Symposium on Contamination Control (ICCCS 90), pp. 14–19.
21. Zhao, J., Shao, X., Li, X., Liang, C., Wang, H., and Xu, W. (2021). Theoretical expression for clean air volume in cleanrooms with non-uniform environments. Build. Environ. *204*, 108168. https://doi.org/10.1016/j.buildenv.2021.108168.
22. Xu, Z. (2014). Principle of cleanroom. In Fundamentals of Air Cleaning Technology and its Application in Cleanrooms (Springer), pp. 377–465. https://doi.org/10.1007/978-3-642-39374-7_8.
23. Yang, L., and Eng Gan, C. (2007). Costing small cleanrooms. Build. Environ. *42*, 743–751. https://doi.org/10.1016/j.buildenv.2005.09.010.
24. Liu, K., Hao, M., Li, B., Guan, T., Chen, S., Wang, G., Xie, Y., and Bian, X. (2022). Optimization on flow field in an operational cleanroom subject to kinematic component and structural parameters. J. Build. Eng. *59*, 105152. https://doi.org/10.1016/j.jobe.2022.105152.
25. Nikoopayan Tak, M.S., Bhattacharya, A., Metcalf, A.R., and Mousavi, E. (2023). Cleanroom air quality: combined effects of ventilation rate and

filtration schemes in a laboratory cleanroom. Build. Res. Inf. *51*, 717–729. https://doi.org/10.1080/09613218.2022.2160299.

26. Bhattacharya, A., Nikoopayan Tak, M.S., Shoai-Naini, S., Betz, F., and Mousavi, E. (2023). A systematic literature review of cleanroom ventilation and air distribution systems. Aerosol Air Qual. Res. *23*, 220407. https://doi.org/10.4209/aaqr.220407.
27. Zhao, W., Li, H., and Wang, S. (2022). A comparative analysis on alternative air-conditioning systems for high-tech cleanrooms and their performance in different climate zones. Energy *261*, 125284. https://doi.org/10.1016/j.energy.2022.125284.
28. Kircher, K., Shi, X., Patil, S., and Zhang, K.M. (2010). Cleanroom energy efficiency strategies: modeling and simulation. Energy Build. *42*, 282–289. https://doi.org/10.1016/j.enbuild.2009.09.004.
29. Loomans, M.G.L.C., Ludlage, T.B.J., van den Oever, H., Molenaar, P.C.A., Kort, H.S.M., and Joosten, P.H.J. (2020). Experimental investigation into cleanroom contamination build-up when applying reduced ventilation and pressure hierarchy conditions as part of demand controlled filtration. Build. Environ. *176*, 106861. https://doi.org/10.1016/j.buildenv.2020.106861.
30. van der Giesen, C., Cucurachi, S., Guinée, J., Kramer, G.J., and Tukker, A. (2020). A critical view on the current application of LCA for new technologies and recommendations for improved practice. J. Clean. Prod. *259*, 120904. https://doi.org/10.1016/j.jclepro.2020.120904.
31. Herrmann, I.T., Hauschild, M.Z., Sohn, M.D., and Mckone, T.E. (2014). Confronting uncertainty in life cycle assessment used for decision support: developing and proposing a taxonomy for LCA studies. J. Ind. Ecol. *18*, 366–379. https://doi.org/10.1111/jiec.12085.
32. Piccinno, F., Hischier, R., Seeger, S., and Som, C. (2016). From laboratory to industrial scale: a scale-up framework for chemical processes in life cycle assessment studies. J. Clean. Prod. *135*, 1085–1097. https://doi.org/10.1016/j.jclepro.2016.06.164.
33. Dahiya, S., Katakojwala, R., Ramakrishna, S., and Mohan, S.V. (2020). Biobased products and life cycle assessment in the context of circular economy and sustainability. Mater. Circ. Econ. *2*, 7. https://doi.org/10.1007/s42824-020-00007-x.
34. Cucurachi, S., Van Der Giesen, C., Guinée, J., and Guineé, J.B. (2018). Ex-ante LCA of emerging technologies. CIRP Procedia *69*, 463–468. https://doi.org/10.1016/j.procir.2017.11.005.
35. Buyle, M., Audenaert, A., Billen, P., Boonen, K., and Van Passel, S. (2019). The future of ex-ante LCA? Lessons learned and practical recommendations. Sustainability *11*, 1–24. https://doi.org/10.3390/su11195456.
36. Arvidsson, R., Svanström, M., Sandén, B.A., Thonemann, N., Steubing, B., and Cucurachi, S. (2024). Terminology for future-oriented life cycle assessment: review and recommendations. Int. J. Life Cycle Assess. *29*, 607–613. https://doi.org/10.1007/s11367-023-02265-8.
37. Pesonen, H.-L., Ekvall, T., Fleischer, G., Huppes, G., Jahn, C., Klos, Z.S., Rebitzer, G., Sonnemann, G.W., Tintinelli, A., Weidema, B.P., et al. (2000). Framework for scenario development in LCA. Int. J. Life Cycle Assess. *5*, 21–30.
38. Cucurachi, S., van der Giesen, C., and Guinée, J. (2018). Ex-ante LCA of emerging technologies. Procedia CIRP *69*, 463–468.
39. Porumb, V.-A., Maier, G., and Anghel, I. (2020). The impact of building location on green certification price premiums: evidence from three European countries. J. Clean. Prod. *272*, 122080. https://doi.org/10.1016/j.jclepro.2020.122080.
40. Díaz-López, C., Jódar, J., Verichev, K., Rodríguez, M.L., Carpio, M., and Zamorano, M. (2021). Dynamics of changes in climate zones and building energy demand. A case study in Spain. Appl. Sci. *11*, 4261. https://doi.org/10.3390/app11094261.
41. Walsh, A., Cóstola, D., and Labaki, L.C. (2022). Performance-based climatic zoning method for building energy efficiency applications using cluster analysis. Energy *255*, 124477. https://doi.org/10.1016/j.energy.2022.124477.
42. IEST-RP-CC012.1 (1993). Considerations in Cleanroom Design. IEST Recommended Practice 012.1 (IEST-RP-CC012.1) (The Institute of Environmental Sciences and Technology (IEST)).
43. Xu, T., and Tschudi, W.F. (2001). Energy performance of cleanroom environmental systems. In ESTECH 2002 Conference.
44. Williams, E., Krishnan, N., and Boyd, S. (2011). Ultrapurity and energy use: case study of semiconductor manufacturing. In Thermodynamics and the Destruction of Resources (Cambridge University Press), pp. 190–211. https://doi.org/10.1017/CBO9780511976049.011.
45. Ludlage, T.B.J., Loomans, M.G.L.C., van den Oever, H., Molenaar, P.C.A., Kort, H.S.M., and Joosten, P.H.J. (2021). Significant energy-saving potential in cleanrooms within reach: A Green deal for cleanrooms. TVVL Mag. *3*, 26–33.
46. De Rosa, M., Bianco, V., Scarpa, F., and Tagliafico, L.A. (2014). Heating and cooling building energy demand evaluation; A simplified model and a modified degree days approach. Appl. Energy *128*, 217–229. https://doi.org/10.1016/j.apenergy.2014.04.067.
47. Beck, H.E., Zimmermann, N.E., McVicar, T.R., Vergopolan, N., Berg, A., and Wood, E.F. (2018). Present and future köppen-geiger climate classification maps at 1-km resolution. Sci. Data *5*, 180214. https://doi.org/10.1038/sdata.2018.214.
48. Hu, S.-C., and Chuah, Y.K. (2003). Power consumption of semiconductor fabs in Taiwan. Energy *28*, 895–907. https://doi.org/10.1016/S0360-5442(03)00008-2.
49. Tsao, J.-M., Hu, S.-C., Xu, T., and Chan, D.Y.L. (2010). Capturing energy-saving opportunities in make-up air systems for cleanrooms of high-technology fabrication plant in subtropical climate. Energy Build. *42*, 2005–2013. https://doi.org/10.1016/j.enbuild.2010.06.009.
50. Chuang, A.C.T. (2008). An Optimized LEED's Green FAB at TSMC. https://www.irbnet.de/daten/iconda/CIB_DC25553.pdf.
51. Ritchie, H., and Roser, M. (2023). Energy Country Profile. https://ourworldindata.org/energy/country/taiwan.
52. Taiwan Semiconductor Manufacturing Company, Ltd. (2023). TSMC 2022 Annual Report. https://investor.tsmc.com/static/annualReports/2023/english/index.html.
53. Energy Administration (2023). 2022 Energy Consumption - Taiwan. https://www.moeaea.gov.tw/ECW/populace/content/Content.aspx?menu_id=14436.
54. Isaac, M., and van Vuuren, D.P. (2009). Modeling global residential sector energy demand for heating and air conditioning in the context of climate change. Energy Policy *37*, 507–521. https://doi.org/10.1016/j.enpol.2008.09.051.
55. Pachauri, R.K., and Meyer, L.A. (2014). IPCC, 2014: Climate Change 2014: Synthesis Report. Contribution of Working Groups I, II and III to the Fifth Assessment Report of the Intergovernmental Panel on Climate Change. https://www.ipcc.ch/site/assets/uploads/2018/05/SYR_AR5_FINAL_full_wcover.pdf.
56. Masson-Delmotte, V., Zhai, P., Pirani, A., Connors, S.L., Péan, C., Berger, S., Caud, N., Chen, Y., Goldfarb, L., Gomis, M.I., et al. (2021). IPCC, 2021: Climate Change 2021: The Physical Science Basis. Contribution of Working Group I to the Sixth Assessment Report of the Intergovernmental Panel on Climate Change. https://www.ipcc.ch/report/ar6/wg1/downloads/report/IPCC_AR6_WGI_SPM_final.pdf.
57. Zhao, Y., Li, N., Tao, C., Chen, Q., and Jiang, M. (2021). A comparative study on energy performance assessment for HVAC systems in high-tech fabs. J. Build. Eng. *39*, 102188. https://doi.org/10.1016/j.jobe.2021.102188.
58. Hu, S.-C., Tsai, Y.-W., Fu, B.-R., and Chang, C.-K. (2017). Assessment of the SEMI energy conversion factor and its application for semiconductor and LCD fabs. Appl. Therm. Eng. *121*, 39–47. https://doi.org/10.1016/j.applthermaleng.2017.04.044.

59. Lin, T., Zargar, O.A., Kalkan, H., Mallillin, A., Hu, S.-C., and Leggett, G. (2020). Energy consumption reduction of a high-tech FAB in Taiwan. J. Energy Dev. *46*, 195–218.

60. Ludlage, T.B.J. (2019). Optimizing energy demand during the non-operational hours in a cleanroom. https://pure.tue.nl/ws/portalfiles/portal/136263172/Ludlage_0964491.pdf.

61. Shan, K., and Wang, S. (2017). Energy efficient design and control of cleanroom environment control systems in subtropical regions – A comparative analysis and on-site validation. Appl. Energy *204*, 582–595. https://doi.org/10.1016/j.apenergy.2017.07.050.

62. Díaz-López, C., Verichev, K., Holgado-Terriza, J.A., and Zamorano, M. (2021). Evolution of climate zones for building in Spain in the face of climate change. Sustain. Cities Soc. *74*, 103223. https://doi.org/10.1016/j.scs.2021.103223.

63. Blanco, C.F., Cucurachi, S., Guinée, J.B., Vijver, M.G., Peijnenburg, W.J.G.M., Trattnig, R., and Heijungs, R. (2020). Assessing the sustainability of emerging technologies: A probabilistic LCA method applied to advanced photovoltaics. J. Clean. Prod. *259*, 120968. https://doi.org/10.1016/j.jclepro.2020.120968.

64. Jusselme, T., Rey, E., and Andersen, M. (2018). An integrative approach for embodied energy: towards an LCA-based data-driven design method. Renew. Sustain. Energy Rev. *88*, 123–132. https://doi.org/10.1016/j.rser.2018.02.036.

65. Heijungs, R., Guinée, J.B., Mendoza Beltrán, A., Henriksson, P.J.G., and Groen, E. (2019). Everything is relative and nothing is certain. Toward a theory and practice of comparative probabilistic LCA. Int. J. Life Cycle Assess. *24*, 1573–1579. https://doi.org/10.1007/s11367-019-01666-y.

66. Pan, T., and Wang, W. (2011). From cleanroom to desktop: emerging micro-nanofabrication technology for biomedical applications. Ann. Biomed. Eng. *39*, 600–620. https://doi.org/10.1007/s10439-010-0218-9.

67. Maltais, T., White, L., Boeder, P., Arakelian, T., Anderson, M., Mennella, J., Heinz, N., Gomez, V., and Chen, N. (2020). Preparing for Mars 2020 and future space missions: technology advancements driving contamination control requirements and cleanroom protocols. In Systems Contamination: Prediction, Control, and Performance 2020, C.E. Soares, E.M. Wooldridge, and B.A. Matheson, eds. (SPIE), p. 27. https://doi.org/10.1117/12.2581239.

68. Wernet, G., Bauer, C., Steubing, B., Reinhard, J., Moreno-Ruiz, E., and Weidema, B. (2016). The ecoinvent database version 3 (part I): overview and methodology. Int. J. Life Cycle Assess. *21*, 1218–1230. https://doi.org/10.1007/s11367-016-1087-8.

69. Steubing, B., de Koning, D., Haas, A., and Mutel, C.L. (2020). The Activity Browser — an open source LCA software building on top of the brightway framework. Software impacts. Software Impacts *3*, 100012. https://doi.org/10.1016/j.simpa.2019.100012.

70. Ritchey, T. (2013). General Morphological Analysis: A General Method for Non-quantified Modelling (Swedish Morphological Society), pp. 1–10.

71. Ritchey, T. (2018). General morphological analysis as a basic scientific modelling method. Technol. Forecast Soc. Change *126*, 81–91. https://doi.org/10.1016/j.techfore.2017.05.027.

72. Ritchey, T. (2015). Principles of cross-consistency assessment in general morphological modelling. Acta Morphol. Gen. *4*, 1–20.

73. Schropp, E., Naumann, G., and Gaderer, M. (2022). Prospective life cycle assessment: a case study of hydrogen production with water electrolysis. Procedia CIRP *105*, 92–97. https://doi.org/10.1016/j.procir.2022.02.016.

74. Delpierre, M., Quist, J., Mertens, J., Prieur-Vernat, A., and Cucurachi, S. (2021). Assessing the environmental impacts of wind-based hydrogen production in the Netherlands using ex-ante LCA and scenarios analysis. J. Clean. Prod. *299*, 126866. https://doi.org/10.1016/j.jclepro.2021.126866.

75. Álvarez, A., and Ritchey, T. (2015). Applications of general morphological analysis. Acta Morphol. Gen. *4*, 1–40.

76. Vutla, S.R., Regalla, S.P., and Ramaswamy, K. (2021). Life cycle assessment of cleanroom for micro-electro-mechanical systems fabrication with insights on sustainability. J. Clean. Prod. *282*, 124520. https://doi.org/10.1016/j.jclepro.2020.124520.

77. Stehfest, E., van Vuuren, D., Kram, T., Bouwman, L., Alkemade, R., Bakkenes, M., Biemans, H., Bouwman, A., den Elzen, M., Janse, J., et al. (2014). Integrated assessment of global environmental change with IMAGE 3.0. Model description and policy applications. https://www.pbl.nl/sites/default/files/downloads/pbl-2014-integrated_assessment_of_global_environmental_change_with_image30_735.pdf.

78. WorldClim (2022). Future climate, 10 minutes spatial resolution. © Copyright 2020–2022. https://www.worldclim.org/data/cmip6/cmip6_clim10m.html.

79. O'Neill, B.C., Kriegler, E., Riahi, K., Ebi, K.L., Hallegatte, S., Carter, T.R., Mathur, R., and van Vuuren, D.P. (2014). A new scenario framework for climate change research: the concept of shared socioeconomic pathways. Clim. Change *122*, 387–400. https://doi.org/10.1007/s10584-013-0905-2.

80. van Vuuren, D.P., Edmonds, J., Kainuma, M., Riahi, K., Thomson, A., Hibbard, K., Hurtt, G.C., Kram, T., Krey, V., Lamarque, J.-F., et al. (2011). The representative concentration pathways: an overview. Clim. Change *109*, 5–31. https://doi.org/10.1007/s10584-011-0148-z.

81. O'Neill, B.C., Tebaldi, C., Van Vuuren, D.P., Eyring, V., Friedlingstein, P., Hurtt, G., Knutti, R., Kriegler, E., Lamarque, J.F., Lowe, J., et al. (2016). The scenario model intercomparison project (ScenarioMIP) for CMIP6. Geosci. Model Dev. *9*, 3461–3482. https://doi.org/10.5194/gmd-9-3461-2016.

82. Mendoza Beltran, A., Cox, B., Mutel, C., van Vuuren, D.P., Font Vivanco, D., Deetman, S., Edelenbosch, O.Y., Guinée, J., and Tukker, A. (2020). When the background matters: using scenarios from integrated assessment models in prospective life cycle assessment. J. Ind. Ecol. *24*, 64–79. https://doi.org/10.1111/jiec.12825.

83. Steubing, B., and de Koning, D. (2021). Making the use of scenarios in LCA easier: the superstructure approach. Int. J. Life Cycle Assess. *26*, 2248–2262. https://doi.org/10.1007/s11367-021-01974-2.

84. Sacchi, R., Terlouw, T., Siala, K., Dirnaichner, A., Bauer, C., Cox, B., Mutel, C., Daioglou, V., and Luderer, G. (2022). PRospective EnvironMental Impact asSEment (premise): A streamlined approach to producing databases for prospective life cycle assessment using integrated assessment models. Renew. Sustain. Energy Rev. *160*, 112311. https://doi.org/10.1016/j.rser.2022.112311.

85. ISO-15927-6 (2007). Hygrothermal Performance of Buildings – Calculation and Presentation of Climatic Data - Part 6: Accumulated Temperature Differences (Degree-Days) (International Organization for Standardization).

86. Spinoni, J., Vogt, J., and Barbosa, P. (2015). European degree-day climatologies and trends for the period 1951–2011. Int. J. Climatol. *35*, 25–36. https://doi.org/10.1002/joc.3959.